SPATIAL INDICATORS OF ECOLOGICAL CONDITION FOR LAKE EYRE BASIN

Ramesh Raja Segaran, Kenneth Clarke, Davina White and Megan Lewis

Goyder Institute for Water Research
Technical Report Series No. 15/30

www.goyderinstitute.org

Goyder Institute for Water Research Technical Report Series ISSN: 1839-2725

The Goyder Institute for Water Research is a partnership between the South Australian Government through the Department of Environment, Water and Natural Resources, CSIRO, Flinders University, the University of Adelaide and the University of South Australia. The Institute will enhance the South Australian Government's capacity to develop and deliver science-based policy solutions in water management. It brings together the best scientists and researchers across Australia to provide expert and independent scientific advice to inform good government water policy and identify future threats and opportunities to water security.

The following Associate organisations contributed to this report:

Enquires should be addressed to: Goyder Institute for Water Research
Level 4, 33 King William Street
Adelaide, SA, 5000
tel: 08-8236 5200
e-mail: enquiries@goyderinstitute.org

Citation

Raja Segaran, R., Clarke, K., White, D and Lewis, M.M. 2015, *Spatial Indicators of Ecological Condition for Lake Eyre Basin.* Goyder Institute for Water Research Technical Report Series No. 15/30, Adelaide, South Australia.

Acknowledgements

The authors wish to acknowledge the contribution of Norman Mueller and Alexis McIntyre of Geoscience Australia, Matthew Miles of DEWNR and Bernie Cockayne of the Queensland Department of Natural Resource Management. Noman Mueller's contribution of his time and the WOfS and WOFLS datasets were invaluable to this project. Matt Miles provided helpful feedback and direction in the collection of data and metadata. Bernie Cockayne was kind enough to deliver access to long-lost waterhole mapping in the Cooper Basin.

The reviewers of this technical report, Dr Justin Costelloe and Assoc. Prof. Bertram Ostendorf, are acknowledged for their constructive suggestions which have helped improve the final report.

Glossary and Definition of Acronyms and Terms

DGPS	Differential Global Positioning System
Endmember	Pure spectral signature which represents a particular material, such as a specific plant type, soil type, or water
GDE	Groundwater Dependent Ecosystem
GIS	Geographic Information System
HyMap	An airborne hyperspectral image sensor operated by HyVista Corporation
Hyperspectral	Imagery or ground data derived from measurements in numerous (more than 10) very narrow bandwidths of the electromagnetic spectrum
LEB	Lake Eyre Basin
MESMA	Multiple Endmember Spectral Mixture Analysis
MODIS	Moderate Resolution Imaging Spectrometer
NDVI	Normalised Difference Vegetation Index
SMA	Spectral Mixture Analysis
WOfS	Water Observations from Space
WOFL	Water Observation Feature Layers

Executive Summary

This report presents research conducted as part of Goyder Institute Project I.2.3 *"Researching environmental condition indicators to support the management of Lake Eyre Basin Rivers".* Aims of the overall project were to research and develop scientific indicators of environmental condition for the aquatic ecosystems of the Lake Eyre Basin (LEB).

The research in this report (conducted as Task 3a within Project I.2.3) focussed on the analysis and integration of ecological and spatial data to develop new methods and indicators of environmental condition for the LEB. It draws on spatially-comprehensive satellite and airborne remote sensing, long time series of frequent, consistent observations and the power of geographic analysis to provide new, objective evidence about the geographic and temporal variability of LEB ecosystems, distribution of ecological indicators and interconnection and function of riverine systems. In addition to providing new understanding of LEB systems, the research has developed and demonstrated several new methods and indicators of ecosystem condition and function that show potential for further development and application within the Basin.

The geographic distribution and temporal response of vegetation growth in terrestrial and aquatic ecosystems in the South Australian LEB has been documented using a fifteen year series of frequent satellite records. This provides new understanding of how vegetation across the Basin functions and responds to rainfall and flood water, and identifies geographic areas that behave similarly. Of particular interest is the finding that vegetation growth in the rivers in the western part of the Basin differs in magnitude and timing from those of the eastern Basin, being fed by rainfall and flood pulses of different origin. In the eastern Basin, the vegetation response of the Georgina and Diamantina Rivers is distinct from that of the Cooper Creek and Coongie Lakes complex, while the Upper Cooper, Cooper flood plain and Coongie Lakes all have different inundation and vegetation greening patterns.

An image-based approach for detecting and mapping the distribution of dominant tree species that are considered potential indicators of long-term reliable riverine flows or of near-surface groundwater is demonstrated. This research focussed on a study area within Arckaringa Creek, using potential differences in the reflectance signatures of the trees as recorded in airborne hyperspectral imagery and *in-situ* spectral measurements. Subject to wider testing with more comprehensive on-ground spectral and botanical sampling, this approach shows potential for development as a method for survey and monitoring of key plant indicators of ecological condition in the LEB.

Spatially explicit visualisations and analysis tools are used to provide insight into the landscape processes that have resulted in the current genetic composition of selected fish populations within LEB. Geographic analyses and applications of new spatial data products are demonstrated to relate environmental processes to biotic connectivity in the LEB. Indicators of hydrologic function are developed from remote sensing and GIS analyses for comparison with results on population genomics of Golden Perch (*Macquaria ambigua*).

The potential of a new satellite remote sensing mapping product is further explored to document the inundation status of selected waterholes within the Neales-Peake River catchment. Due to the remote and extensive geography of the Lake Eyre Basin, gaining an overview of the persistence of inundation in fish refugia has been problematic. Here a long series of records of surface inundation derived from satellite images was interrogated to provide new evidence of waterhole persistence at the end of long dry periods. The results show that only 11% of waterholes retained water through four droughts since 1999, more than half were dry at the end of all four periods, while around 40% showed different responses after each dry

period. This information helps identify core wetlands that are likely to be critical for long term species survival and can inform broader management of aquatic ecosystems in the LEB.

Benefits that can be gained from integrating spatial analysis and visualisation with traditional field sampling studies are also demonstrated. Results from a water quality sampling campaign throughout upper reaches of eastern LEB rivers are presented in a website that hosts a facility for interactive display in Google Earth. The site serves as a pilot demonstration of development of open data sharing to encourage public interest and to make the information accessible to collaborating organisations.

There are considerable benefits in developing these new approaches to encompass wider parts of the LEB, and in interpreting the new spatially-explicit indicators of ecological function and condition in conjunction with results from other environmental studies in the Basin. The new landscape classifications based on riverine inundation and vegetation response provide a fuller spatiotemporal context for interpreting sparse and diverse ecological data and could direct future on-ground sampling to achieve better spatial and temporal representation. Several of the indicators presented here help define envelopes of natural variability for unmodified LEB rivers, which with further analysis could reveal underlying climatic trends and influences. This understanding of natural spatial and temporal variability of water and vegetation within the LEB also defines the conditions against which potential impacts from anthropogenic changes may be identified.

Contents

Figures

Tables

1. Introduction

This report presents research conducted as part of Goyder Institute Project I.2.3 *"Researching environmental condition indicators to support the management of Lake Eyre Basin Rivers".* Aims of the overall project were to research and develop scientific indicators of environmental condition for the aquatic ecosystems of the Lake Eyre Basin (LEB). The indicators and methods developed during this project may be used to inform the assessment of environmental condition of LEB rivers as required under the LEB Intergovernmental Agreement (LEBIA) to which South Australia is a signatory.

Determining condition, monitoring change and assessing potential impacts of anthropogenic activities all require an understanding of the natural variability of the highly dynamic aquatic and dry land ecosystems within the LEB. Yet to date most of information about these ecosystems comes from sparsely distributed, often intermittent observations and physical and biological samples. While this information has provided a foundation for conceptual models of ecosystem and biological function in LEB rivers, it is generally insufficient to enable reliable comparisons of widely separated geographic regions or assessment of trends over time.

The research in this report (conducted as Task 3a within Project I.2.3) focussed on the analysis and integration of ecological and spatial data to develop new methods and indicators of environmental condition for the LEB. It draws on spatially-comprehensive satellite and airborne remote sensing, long time series of frequent, consistent observations and the power of geographic analysis to provide new, objective evidence about the geographic and temporal variability of LEB ecosystems, distribution of ecological indicators and interconnection and function of riverine systems. In addition to providing new understanding of LEB systems, the research has developed and demonstrated several new methods and indicators of ecosystem condition and function that show potential for further development and application within the Basin.

The research was conducted as a series of studies at different geographic scales: some basin-wide, and others focussed on case study areas determined by availability of *in-situ* or existing data for comparison. These studies are reported in the following sections of this report.

Section 2 characterises the geographic distribution and temporal response of vegetation growth in terrestrial and aquatic ecosystems in the South Australian LEB, using a fifteen year series of frequent satellite records. This provides new understanding of how vegetation across the Basin functions and responds to rainfall and flood water, and identifies geographic areas that behave similarly.

Section 3 demonstrates an new image-based approach for detecting and mapping the distribution of dominant tree species that are considered indicators of long-term reliable riverine flows or of near-surface groundwater in the LEB. This research focussed on a study area within Arckaringa Creek, using potential differences in the reflectance signatures of the trees as recorded in airborne hyperspectral imagery and *in-situ* spectral measurements.

Section 4 uses spatially explicit visualisations and analysis tools to provide insight into the landscape processes that have resulted in the current genetic composition of selected fish populations within LEB. The study demonstrates geographic analyses and applications of new spatial data products to relate environmental processes to biotic connectivity in the LEB. Indicators of hydrologic function are developed from remote sensing and GIS analyses for comparison with results on population genomics of Golden Perch (*Macquaria ambigua*).

Section 5 explores the potential of a new satellite remote sensing mapping product to document the inundation status of selected waterholes within the Neales-Peake River catchment. Because of the remote and extensive geography of the Lake Eyre Basin, gaining an overview of the persistence of inundation in fish refugia has been difficult. Here a long series of records of surface inundation derived from satellite images was interrogated to provide new evidence of waterhole persistence at the end of long dry periods.

Finally, section 6 demonstrates benefits that can be gained from integrating spatial analysis and visualisation with traditional field sampling studies. Results from a water quality sampling campaign throughout upper reaches of eastern LEB rivers are presented in a website that hosts a facilty for interactive display in Google Earth. The site serves as a pilot demonstration of development of open data sharing to encourage public interest and to make the information accessible to collaborating organisations.

2. Basin-scale greenness and phenology indicators of ecosystem response

2.1 Introduction

The aim of the research presented in this section was to characterise the geographic distribution and temporal response of vegetation growth in terrestrial and aquatic ecosystems in the South Australian Lake Eyre Basin, where vegetation production is thought to be one of the main drivers of ecosystem function. Indeed, Productivity Theory provides an explanation for why total primary productivity is a key determinant of ecosystem function: the greater the amount and duration of primary productivity the greater the capacity to generate and support high biodiversity (O'Brien 1993; Whittaker et al. 2003)

Although the study included all of the LEB in South Australia, it had a special focus on riparian areas dominated by surface flows.

The research achieves several benefits. Firstly, it provides new information on the spatiotemporal vegetation greenness pattern of broad landscapes within the region, improving understanding of how vegetation functions and responds to rainfall and flood water, and identifying geographic areas that behave similarly. This objective evidence of landscape function across the Basin over the past 15 years may also assist development, evaluation and refinement of conceptual models for these ecosystems. In addition, it provides a spatial and temporal context within which to interpret existing and future field data. Currently, much of the field data in the region is from infrequent and sparsely distributed samples, making it difficult to interpret geographic and temporal trends. The landscape stratification provided here should assist interpretation of sparse environmental data and focus future field data collection.

2.2 Methods

The methodology is summarised in the following steps:

- We obtained a satellite-based image measure of vegetation greenness over the study area: this measure is available every two weeks from 2000 to present
- Principal components analysis and an unsupervised clustering process were used to group together pixels of similar temporal greenness and inundation history
- The most similar classes were combined, until further grouping would reduce the number of riparian classes
- The spatial extent of the resulting 16 temporal greenness classes was mapped
- For each temporal greenness class we extracted mean vegetation greenness for all image dates
- We also obtained monthly gridded rainfall data for the study area, and extracted monthly mean rainfall for each temporal greenness class for the study period
- Finally, temporal profiles of vegetation greenness and rainfall were graphed for each of the 16 temporal greenness classes

2.2.1 MODIS NDVI Data

This research used Normalised Difference Vegetation Index (NDVI) data from the Moderate Resolution Imaging Spectroradiometer (MODIS) sensor. The MODIS sensor is on board the Aqua and Terra satellites operated by NASA. The MODIS sensor records reflectance in 36 spectral bands ranging from 0.4 µm to 14.4 µm, and in spatial resolutions ranging from 250 m to 1000 m. Two copies of the instrument are operational at the time of writing, on board the Terra and Aqua polar-orbiting satellites, and each images the entire Earth surface every 1 to 2 days. In addition to supplying raw MODIS reflectance data, NASA produces several highly validated MODIS image products, including the MOD13Q1 vegetation indices product used in this project.

The NDVI index is a measure of vegetation greenness (a combination of total leaf area and per-leaf chlorophyll concentration), and indirectly an index of inundation. The NDVI is based on the contrast between red and near infra-red reflectance. There is a large difference in red and near infra-red reflectance for green vegetation and water, and a smaller difference for other cover types. The index is formulated so that strongly growing vegetation produces high NDVI values, up to 0.8, while dead vegetation or exposed dry soil produce NDVI values of approximately 0.2, and exposed water produces values close to -0.2.

The MOD13Q1 NDVI product used in this project is a composite product, produced from multiple images rather than a single image acquisition, and has a resolution of 250 m. The compositing process evaluates all MODIS imagery of a given area within a 16 day period and assigns each image element (pixel) a quality value, with higher values given to cloud free pixels and pixels near to nadir (looking directly down) view angle. The final composite MODIS image is made up of a weighted average of the best quality pixels over the 16 day period

2.2.2 MODIS pre-processing

Four MODIS scenes were required to cover the study area, and complete temporal coverage from the start of the MODIS archive (18 February 2000) to the end of 2014 required 342 NDVI images, thus, 1368 images in total.

Prior to analysis, all four scenes for each image date were mosaicked into 342 single images covering the whole study area. Due to the wide swath of MODIS, these mosaicked images covered much of Australia. To reduce processing time of future steps, and to ensure that the temporal greenness clustering was based on the temporal greenness of pixels within the study area, pixels outside the study area were masked out, and eliminated from further processing. The study area was defined as the South Australian portion of the LEB.

2.2.3 Rainfall data

The Australian Water Availability Project (AWAP) precipitation product (run 26j) was analysed to provide climatic context and comparison with the vegetation greenness (NDVI) data. This data product is interpolated at a 5 km resolution from Bureau of Meteorology rainfall gauge data. Monthly AWAP data was obtained over the whole study area for the period covered by the MODIS satellite data.

2.2.4 Clustering Analysis

A principal components analysis was performed on all 342 MODIS NDVI image dates, from 2000 to end of 2014, producing 341 principal components (PCs). Examination of the Eigen values revealed that PCs 1 – 49 contained more than 98 % of the information in the dataset, while all remaining PCs contained less than 2 % of the information. Consequently, to eliminate noise, and improve classification quality an ISOCLASS unsupervised classification was run on PCs 1 – 49, producing 49 temporal greenness classes. Next, class similarity and a hierarchical clustering algorithm were used to produce a dendrogram to interpret relationships between the classes (Figure 1). The dendrogram is computed by measuring the distance between each pair of classes, using a measure of distance between class means and variances (Equation 1). Then, iteratively the closest pair of classes are merged, then the next closest pair of classes, and so on until all classes are merged (ArcGIS 10.1 documentation). The distance between pairs of classes, and the sequence of their merging is presented in **Error! Reference source not found.** in Appendix 1.

$$d_{mn} = \sum_{i=1}^{N} \frac{(\mu_{mi} - \mu_{ni})^2}{\sqrt{V_{mi} V_{ni}}} \qquad (1)$$

where:

d is the distance between pairs of classes

m and *n* are the two classes being compared

i is the layer number

μ is the mean of class *m* or *n* in layer *i*

V is the variance of class *m* or *n* in layer *i*

Finally, we iteratively merged pairs of classes in the order computed in creating the dendrogram until further grouping would have merged a riparian class with any other class. This point corresponded to a between-class distance of greater than 5.83, and less than 6.05. Assessment of riparian status was determined by comparison of the class extent with Google Earth imagery, Landsat imagery, and spatial river and stream vector layers for Australia. The final aggregation resulted in 16 classes. Mapping the distribution of the 16 classes was performed by vectorising the ISOCLASS raster classification, then progressively merging polygons as indicated by the dendrogram clustering routine (see table of class pair distances in **Error! Reference source not found.**, Appendix 1).

2.2.5 Temporal greenness profile and monthly rainfall extraction

For the 16 temporal greenness classes mean NDVI (as an indicator of greenness and inundation) was extracted for every image date. Monthly rainfall data was also extracted for each of the sixteen temporal greenness class extents for the period covered by the NDVI data, to provide a climatic context to the temporal greenness profile interpretation. Both NDVI temporal profiles and monthly rainfall data were then graphed.

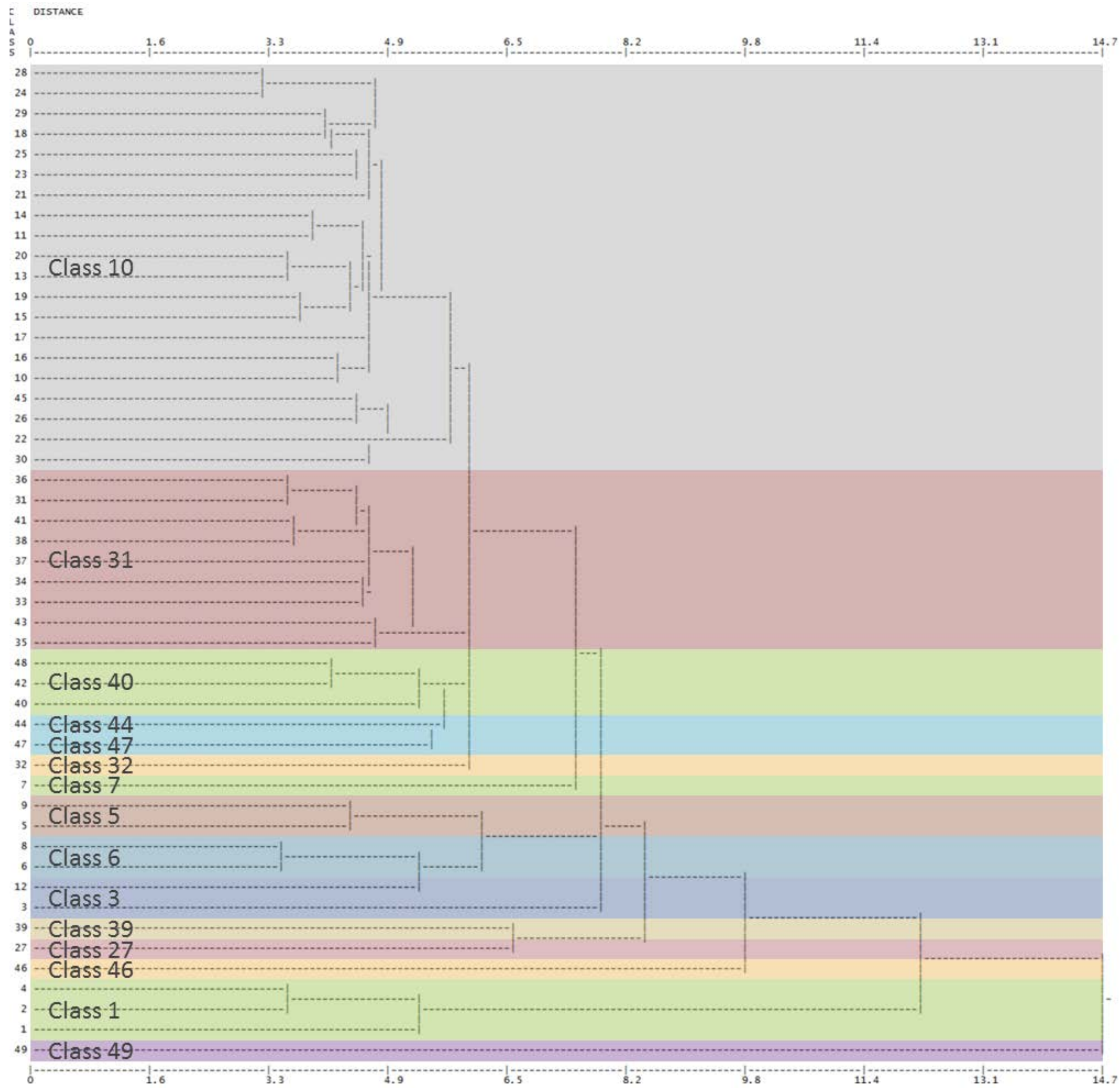

Figure 1. Dendrogram of class similarity. Figure is output from ArcGIS 10.1 Spatial Analyst Dendrogram tool. Final aggregated classes are overlain in colour.

2.3 Results

For each of the 16 distinct temporal greenness classes, this section presents maps of geographic distribution, and graphs of temporal greenness profiles and mean monthly rainfall. These results and their interpretation are prefaced by a guide to interpreting temporal greenness profiles.

2.3.1 Temporal greenness profile interpretation guide

In simple terrestrial systems interpretation of NDVI is relatively straightforward: high NDVI values (around 0.8) correspond to extremely dense, very strongly growing vegetation (e.g., temperate or tropical forest, or full crop canopy), and low values (around 0.15) indicate dead vegetation or bare soil. However, in more complex systems like this where salt crusts (evaporite) or extensive inundation are also present interpretation requires more nuanced. Evaporite can produce NDVI values lower than exposed soil, and extensive inundation can result in NDVI values of 0.0 or lower.

As a guide, NDVI values below 0.1 should be considered indicative of extensive inundation or evaporite, and values above 0.4 indicative of extensive and strong vegetation growth. However, it is essential to remember that these are not exclusive conditions, and an NDVI value below 0.2 does not necessarily mean there is little or no vegetation growth. If all the pixels in a class on a given date contain a mixture of moderately strongly growing vegetation (NDVI = 0.4) and open water (NDVI = 0.0), the observed NDVI will be the mean (NDVI = 0.2). Likewise, NDVI values above 0.4 do not mean that there is no inundation, but instead that the chlorophyll signal is having a greater impact on the observed NDVI than any inundation. In this latter case, extensive inundation may eventually result in strong growth of floating and anchored vegetation which will physically reduce the visible water area, and begin to overwhelm the water effect on NDVI. Thus, it is important to take climatic context when interpreting the temporal greenness profiles.

2.3.2 Clustering

This analysis covered the whole of the South Australian Lake Eyre Basin, and grouped the landscape into areas of similar temporal greenness and inundation history. Class number, spatial distribution, cover type and a brief description are presented in Table 1. For presentation, the classes have been grouped into four sets of four based on similarity of spatial distribution. Maps of the spatial distribution of classes and graphs of temporal greenness profiles and monthly rainfall are presented in four pairs of four classes, with maps and graphs for each set of classes presented on facing pages.

Broadly, four kinds of vegetation greenness response were identified:

- Xeric (dry) or dry-mesic (less dry) rangeland, with little vegetation cover, little growth in response to infrequent rainfall events, and no evidence of inundation: Classes 5, 6, 7, 10, 31, 32, 46 and 47
- Riparian, moderate vegetation cover with periods of very strong probably inundation dependent vegetation growth associated with evidence of significant inundation: 3, 27, 35, 39 and 44
- Strongly seasonal, strong seasonal cycle of growth and senescence in response to strongly seasonal rainfall: Classes 40 and 49
- Evaporation basin, no evidence of vegetation cover, spatially restricted to salt lakes and clay pans: Class 1.

Table 1. Temporal greenness class numbers, geographic distribution, cover type and brief description and interpretation of class temporal greenness response in relation to probable vegetation type, cover, density and dependence on inundation or rainfall. Class numbers derive from the original ISOCLASS unsupervised classification, and the class lumping process (section 2.2.4).

Class number	Spatial Distribution	Cover type	Short temporal greenness description with reference to Class 10, the majority of the rangeland in the region
1	Salt lakes and clay pans	Evaporation basin	Salt lakes and clay pans; lower NDVI than class 10 at all times; no increase in greenness after rainfall, hence no evidence of vegetation.
3	Coongie Lakes	Riparian	Very similar greenness to Class 10, except for several periods of very low NDVI associated with rainfall. The periods of very low NDVI suggest extensive inundation. These periods are occasionally followed by a small increase in greenness, probably minor vegetation growth in response to increased water availability. Sudden decreases in NDVI occur at similar time to the largest increases in greenness in Classes 27 and 39, suggesting that these three classes are responding to the same rainfall or flooding events.
5	Central-western	Xeric rangeland	Lower overall greenness than Class 10, but does respond slightly to rainfall. Suggests presence of sparse rainfall-dependent rangeland vegetation.
6	Central	Xeric rangeland	Lower overall greenness than Class 10, but does respond slightly to rainfall. Suggests presence of sparse rainfall-dependent rangeland vegetation.
7	Central-western	Xeric rangeland	Lower overall greenness than Class 10, but slightly more than Classes 5 and 6, also slightly stronger response to rainfall. Suggests less sparse rainfall-dependent rangeland vegetation than Class 5 and 6.
10	Central	Xeric rangeland	Majority of the study area, low overall greenness with small responses to rainfall events. Typical of a combination of sparse perennial and ephemeral rainfall-dependent rangeland vegetation.
27	Cooper flood plain	Riparian / floodplain	Very similar greenness to Class 10 in dry years, but very large increases in greenness in response to rainfall. No strong decreases in NDVI to suggest extensive inundation. Suggests a combination of rainfall dependant rangeland vegetation, and presence of inundation-dependent vegetation capable of significant growth in response to shallow inundation or topographic concentration of rainfall runoff. Increases in greenness occur at a similar time to – but are smaller than – those seen in Class 39, and correspond to the timing of the sudden decreases in NDVI in Class 3, suggesting these three classes are responding to the same rainfall or flooding events.

Class number	Spatial Distribution	Cover type	Short temporal greenness description with reference to Class 10, the majority of the rangeland in the region
31	Predominantly south-eastern	Xeric rangeland	Similar temporal greenness pattern to Class 10, but higher greenness on all dates, and larger increases in response to rainfall. Suggests denser rainfall dependant rangeland vegetation than Class 10.
32	Simpson Desert	Xeric rangeland	Similar temporal greenness pattern to Class 10, but higher greenness on most dates, and slightly larger increases in response to rainfall. Suggests somewhat denser rainfall dependant rangeland vegetation than Class 10.
35	Georgina and Diamantina	Riparian	Higher greenness than Class 10 in most years. Often very large increases in greenness sometimes associated with rainfall. Occasional sudden decreases in NDVI suggest extensive inundation. Suggests vegetation capable of significant growth in the presence of water, dependent on stream flow resulting from rainfall outside the local area. Similarity of timing of increases and decreases in greenness suggest that this class may be responding to some of the same rainfall or flooding events that feed Classes 3, 27 and 39. However, additional increases (2001 and 2009) and sudden decreases in greenness (2009) suggest that this system receives some additional floodwater from events that do not feed into Classes 3, 27 and 39.
39	Upper Cooper	Riparian	Higher greenness than Class 10 in all years. Often very large increases in greenness sometimes associated with rainfall. Occasional sudden decreases in NDVI suggest extensive inundation. Suggests vegetation capable of significant growth in the presence of water, dependent on stream flow resulting from rainfall outside the local area. Similarity of timing of increases and decreases in greenness suggest that this class is responding to the same rainfall or flooding events that feed Classes 3 and 27, and some of the flooding events that feed Class 35.
40	Flinders Ranges	Dry-mesic woodland dominated ranges	Considerably higher greenness than Class 10 in all years, and much more pronounced and regular seasonal pattern of winder greening and summer senescence. Significant increase in greenness in response to large rainfall events. The high mean and regular seasonality of this temporal greenness pattern suggests perennial vegetation receiving regular winter rainfall from the southern ocean. Spatially, this class is restricted to the Flinders Ranges, which is dominated by perennial vegetation, and receives the majority of its rainfall from rainfall systems that come from the south west.

Class number	Spatial Distribution	Cover type	Short temporal greenness description with reference to Class 10, the majority of the rangeland in the region
44	Western river systems	Riparian	Very similar greenness to Class 10 in dry years, but frequent moderate to large increases in greenness, sometimes associated with rainfall and sometimes not. No sudden decreases in NDVI suggesting extensive inundation. Suggests vegetation capable of significant growth in the presence of water, dependent on stream flow resulting from rainfall outside the local area. Timing and magnitude of increases in greenness do not correspond closely with the other riparian systems (Classes 3, 27, 35 and 39). Suggests that this class receives floodwater from different rainfall events than those that feed Classes 3, 27, 35 and 39.
46	Upper north-west	Dry-mesic rangeland	Wetter than other dryland classes, higher basal greenness; receives more rainfall, and responds with stronger growth
47	Pedirka IBRA sub-region	Dry-mesic rangeland	Similar growth pattern to other dryland classes, but higher mean greenness; suggests that system maintains more vegetation through dry periods than the central and western dryland classes (5, 6, 7, 10, 32), and in wet periods receives more rainfall and produces more vegetation than the other dryland classes
49	South Australian wheat-belt	Mediterranean climate, marginal cropping	Very pronounced seasonal greenness pattern, with very high winter greenness and low summer greenness. The very high amplitude, and regular seasonality of this class is indicative of Mediterranean-climate dominated seasonal cropping. Geographically, this class is the north-eastern margin of the South Australian wheat-belt.

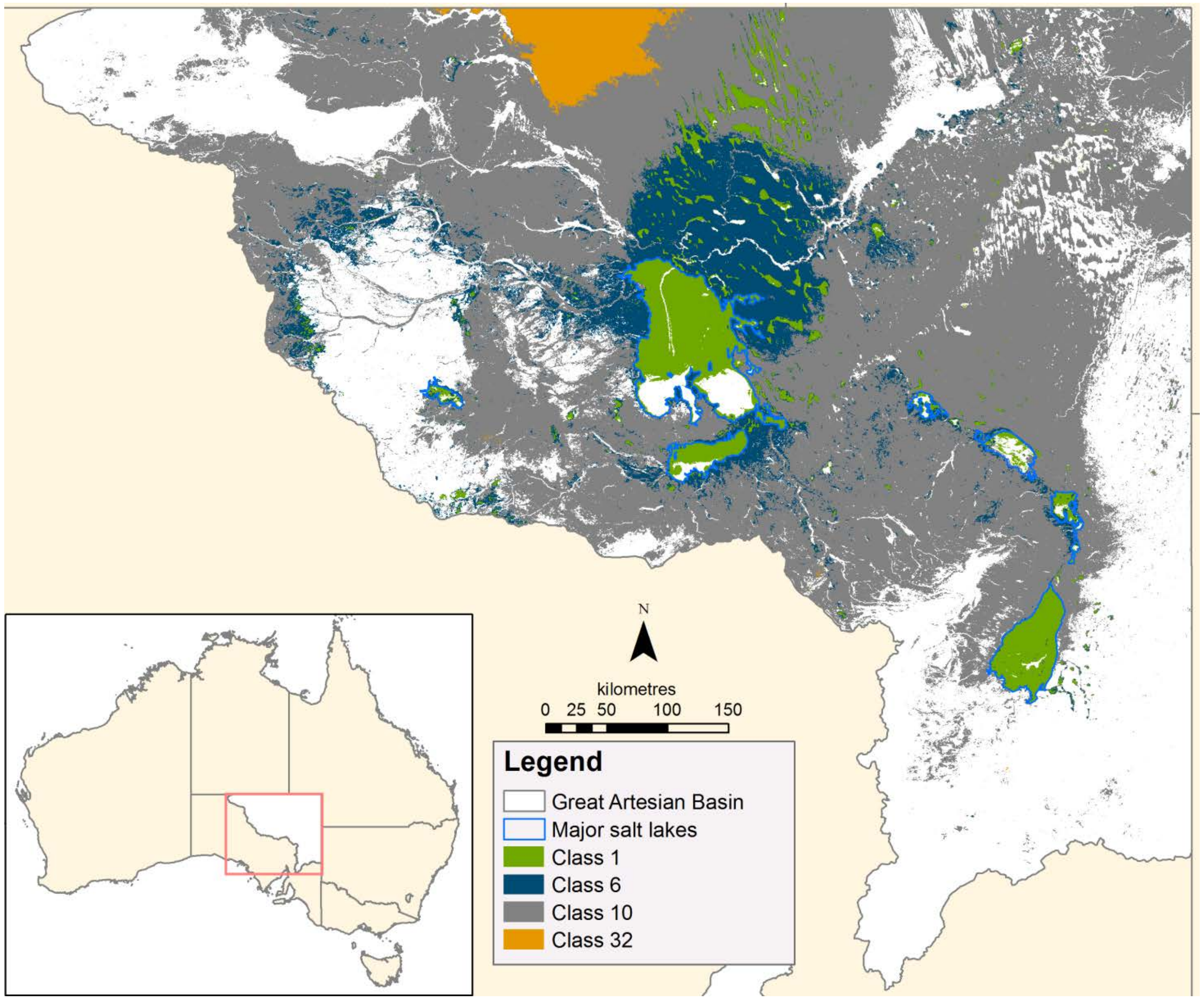

Figure 2. Spatial distribution of temporal greenness Classes 1, 6, 10 and 32. All pixels within each class share a similar temporal greenness pattern (NDVI) over the 2000 to 2014 period. Brief descriptions and interpretation of class temporal greenness response in relation to probable vegetation type, cover, density and dependence on inundation or rainfall are presented in Table 1.

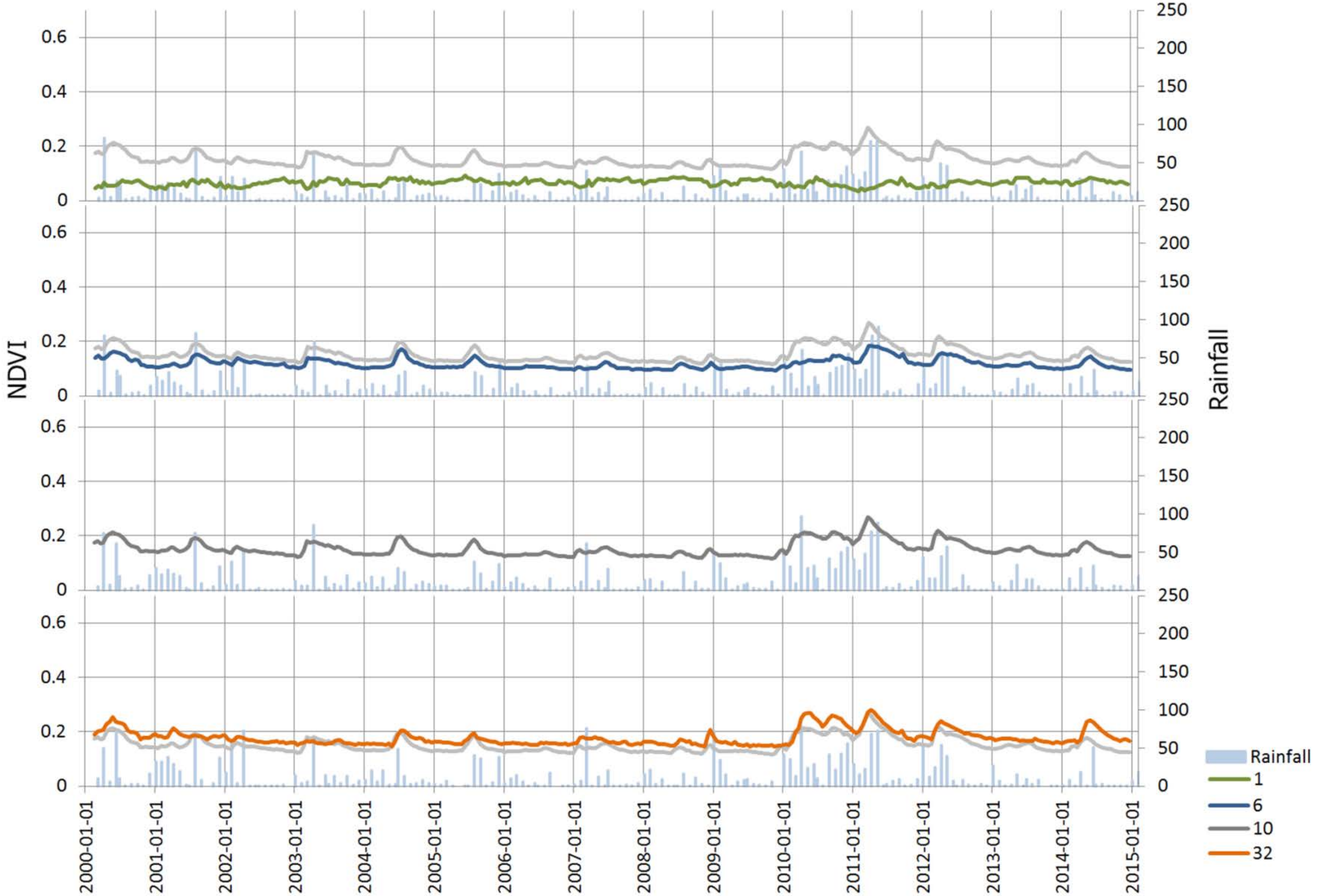

Figure 3. Temporal greenness profile and monthly rainfall for Classes 1, 6, 10 and 32 over the 2000 to 2014 period. The temporal greenness profile for Class 10 is presented in light grey for comparison.

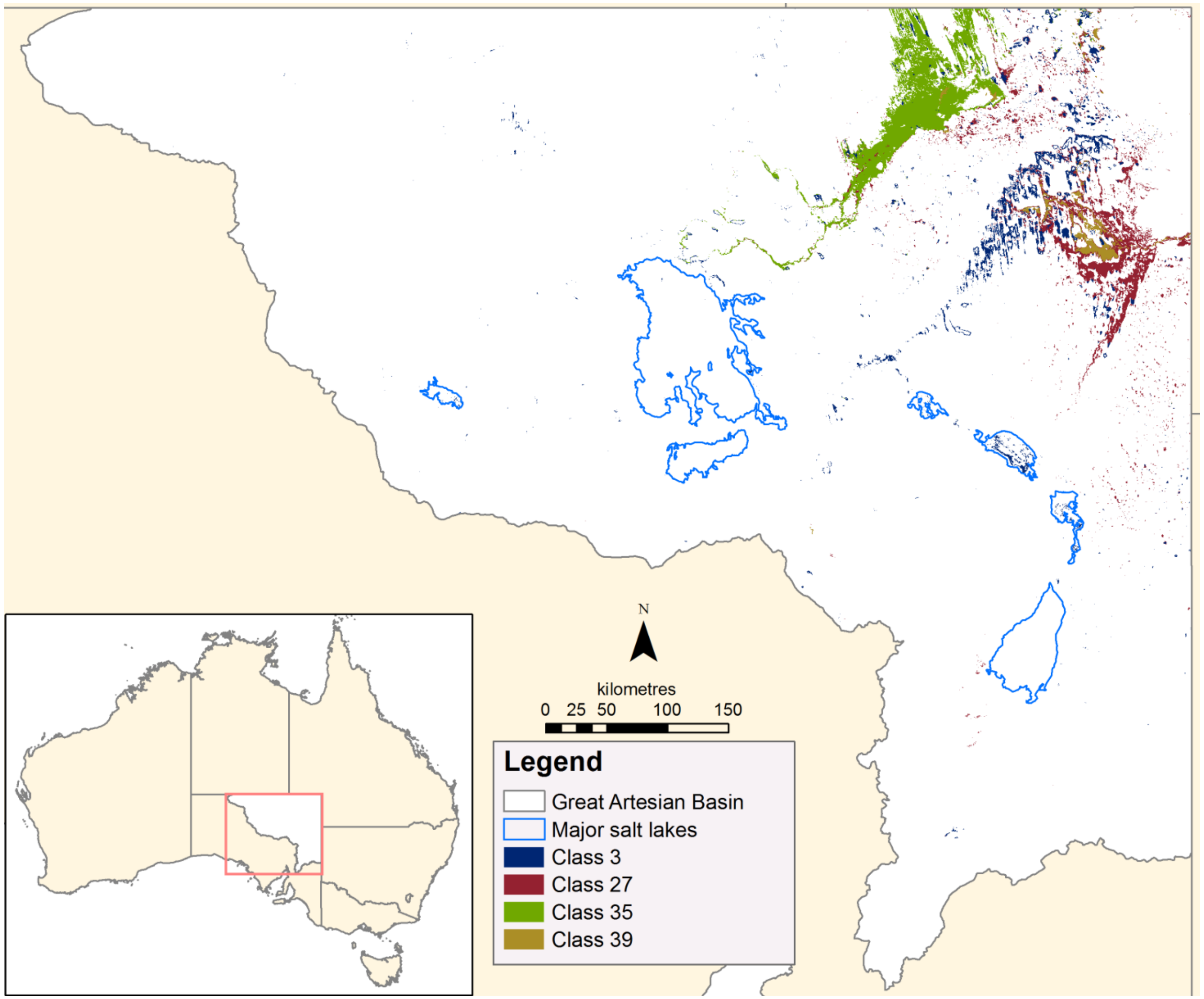

Figure 4. Spatial distribution of temporal greenness Classes 3, 27, 35 and 39. All pixels within each class share a similar temporal greenness pattern (NDVI) over the 2000 to 2014 period. Brief descriptions and interpretation of class temporal greenness response in relation to probable vegetation type, cover, density and dependence on inundation or rainfall are presented in Table 1.

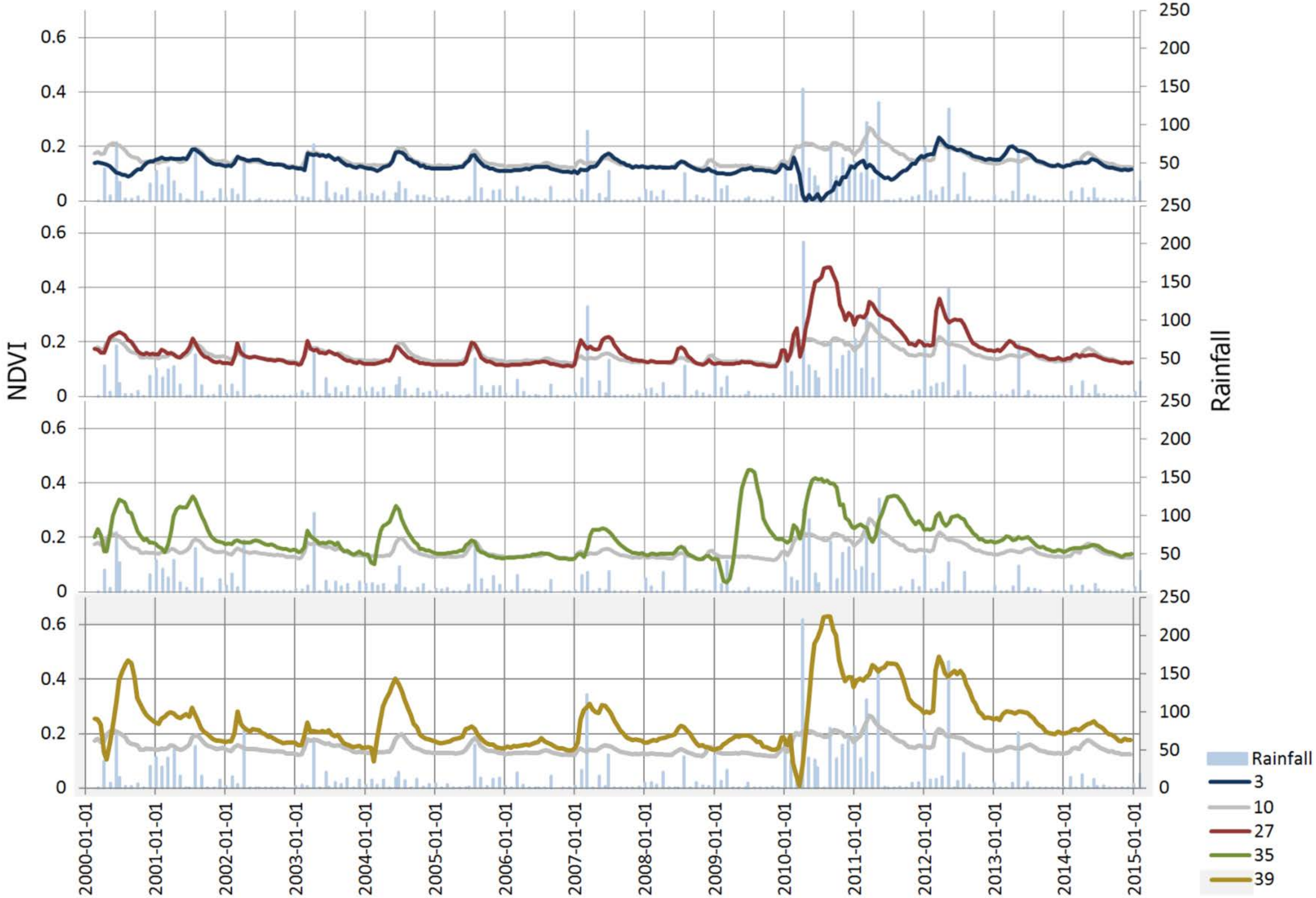

Figure 5. Temporal greenness profile and monthly rainfall for Classes 3, 27, 35 and 39 over the 2000 to 2014 period. The temporal greenness profile for Class 10 is presented in light grey for comparison.

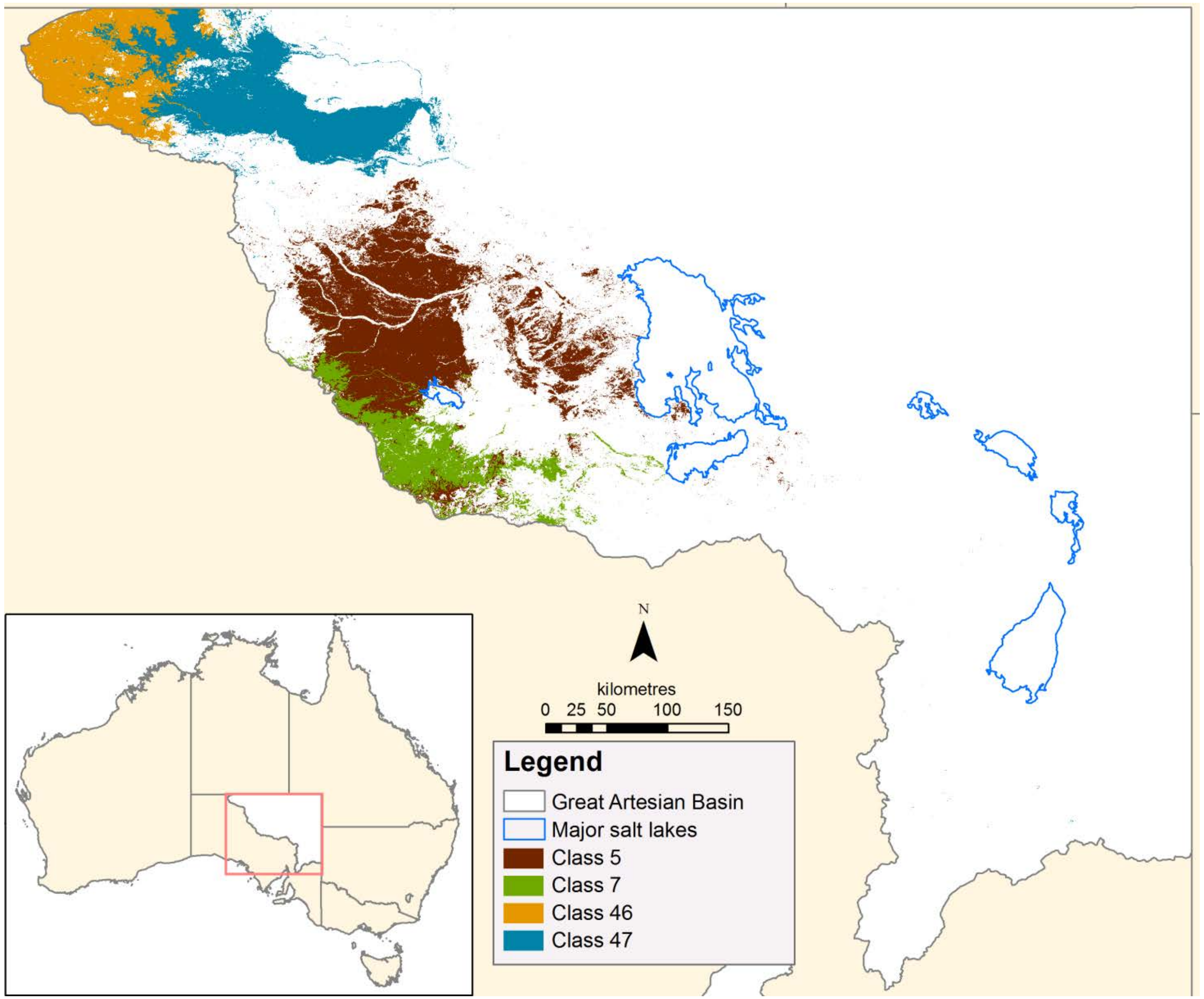

Figure 6. Spatial distribution of temporal greenness Classes 5, 7, 46 and 47. All pixels within each class share a similar temporal greenness pattern (NDVI) over the 2000 to 2014 period. Brief descriptions and interpretation of class temporal greenness response in relation to probable vegetation type, cover, density and dependence on inundation or rainfall are presented in Table 1.

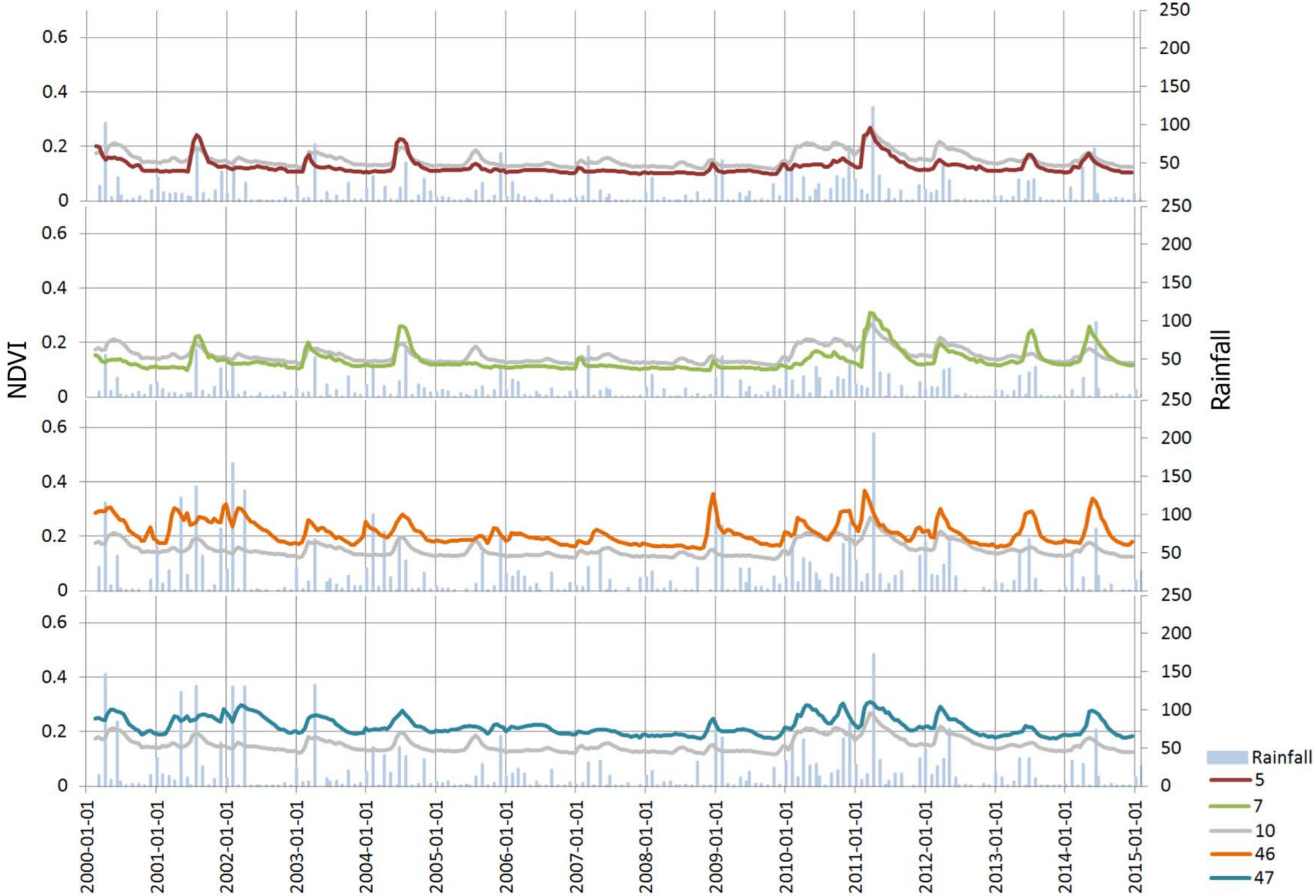

Figure 7. Temporal greenness profile and monthly rainfall for Classes 5, 7, 46 and 47 over the 2000 to 2014 period. The temporal greenness profile for Class 10 is presented in light grey for comparison.

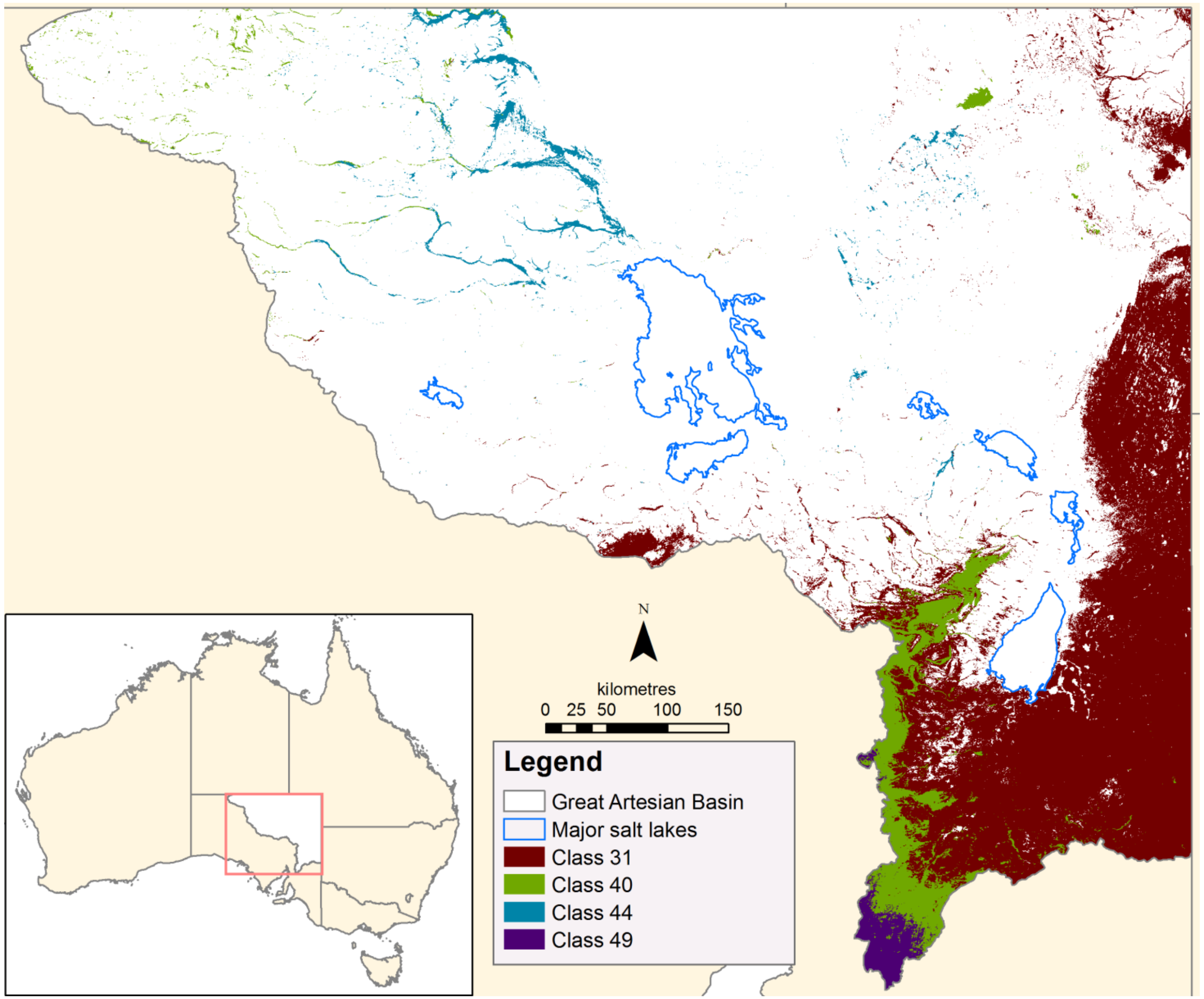

Figure 8. Spatial distribution of temporal greenness Classes 31, 40, 44 and 49. All pixels within each class share a similar temporal greenness pattern (NDVI) over the 2000 to 2014 period. Brief descriptions and interpretation of class temporal greenness response in relation to probable vegetation type, cover, density and dependence on inundation or rainfall are presented in Table 1.

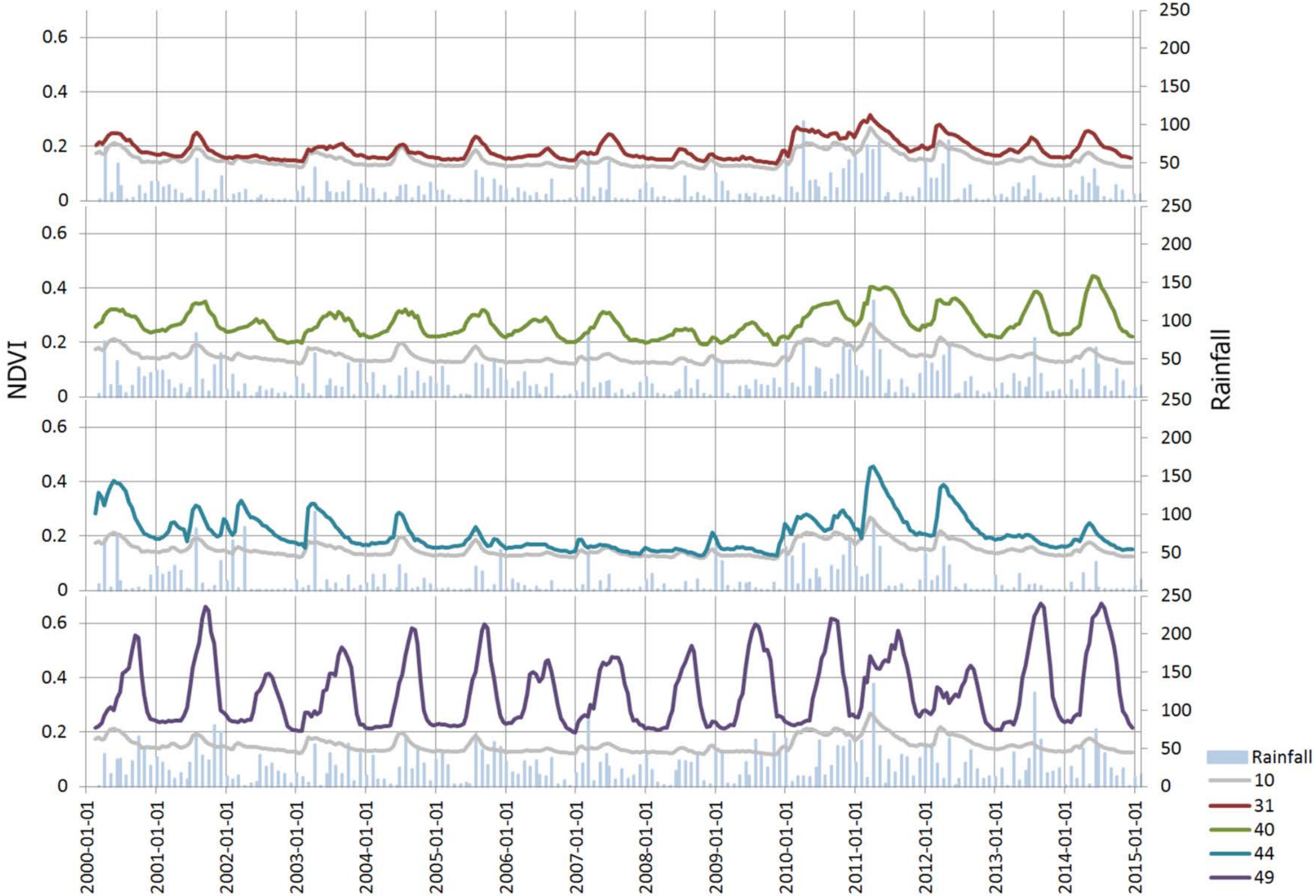

Figure 9. Temporal greenness profile and monthly rainfall for Classes 31, 40, 44 and 49 over the 2000 to 2014 period. The temporal greenness profile for Class 10 is presented in light grey for comparison.

2.4 Discussion

The aim of this research was to characterise the temporal vegetation response of terrestrial and aquatic ecosystems in the South Australian Lake Eyre Basin. Its motivation was to 1) improve understanding of the landscape-scale vegetation dynamics, which is an important step to understanding ecosystem function, and 2) to provide a spatiotemporal context within which to place and understand existing and new field data, and conceptual models.

The South Australian Lake Eyre Basin has been grouped into 16 classes of similar temporal greenness and inundation history. Examination and interpretation of the temporal greenness profiles in relation to rainfall revealed that the classes fell into four broad categories: xeric or dry-mesic rangeland, riparian, strongly seasonal, and evaporation basin.

Given the Goyder Institute's focus on water, the riparian classes (3, 27, 35, 39 and 44) are the most relevant for the current work. However, the surrounding rangeland systems can have a large influence on neighbouring riverine systems, and so the other terrestrial classes are also important. However, the focus of this discussion is on the riparian classes.

Amongst the riparian systems, there are varying degrees of similarity or difference between the classes. Class 44 differs most from the others and is geographically located almost entirely in the western Lake Eyre Basin, whereas the other four riparian classes are located in the east. The timing and magnitude of increases in greenness in class 44 do not correspond closely to any of the other riparian classes, suggesting that this class largely receives floodwater from different rainfall events than the other riparian classes.

The four eastern classes naturally fall into two geographic and temporal greenness groupings. Class 35 geographically coincides with the Georgina and Diamantina rivers, while classes 3, 27 and 39 are all spatially coincident with parts of the Cooper Creek system. Temporally, all four eastern riparian classes show similar timing of increases or decreases in greenness, both of which suggest inundation or vegetation response to inundation in 2000, 2010, 2011 and 2012. Furthermore, the Georgina and Diamantina (class 35) and Upper Cooper (class 39) share evidence of small or moderate inundation or vegetation response to inundation in 2004 and 2007, while class 27 also shows a very small increase in greenness in 2007. Finally, the Georgina and Diamantina class exhibits inundation and following vegetation response in 2009, not evident for the other eastern riparian classes.

Our interpretation of these events is that floodwaters from the same rainfall events sometimes feed into both the Cooper and Georgina and Diamantina systems (e.g., 2000, 2004, 2007, 2010, 2011, and 2012), but that on occasions these floodwaters are not sufficient to extend all the way down the Cooper system to Coongie Lakes (e.g., 2004, 2007), or aren't of sufficient volume to flow onto the Cooper flood plain (e.g., 2004). Additionally, it appears that the Georgina and Diamantina system sometimes receives floodwaters from rainfall events that do not reach the Cooper catchment.

The significance of this finding is that, at least for the period covered by MODIS (2000-2015), it appears that there are three spatiotemporally distinct vegetation greenness and flooding event types within the Cooper system, but that there is only one more-or-less similar response in the Georgina and Diamantina system. Within the Cooper system, the Upper Cooper is inundated and greens more regularly, (evidence of large-scale inundation in 3 out of 15 years, and large increases in greenness probably due to floodwaters in 7 out of 15 years), the Cooper flood plain is inundated and greens less regularly (evidence of large-scale inundation in 1 year, and large increases in greenness in 4 out of 15 years), and Coongie Lakes receives inundation even less frequently (3 out of 15 years), and almost never produces significant vegetation in response to inundation. Within the Georgina and Diamantina system, the mapped extent is inundated and greens very regularly (evidence of large-scale inundation in 5 out of 15 years, and large increases in greenness in 8 out of 15 years), even more so than the Upper Cooper class.

2.5 Conclusions and recommendations

The analysis presented here provides new objective information on broad types of landscape response to rainfall and inundation in the South Australian Lake Eyre Basin. It provides a foundation for improving understanding of how vegetation functions and responds to rainfall and flood water, and identifies areas with similar spatiotemporal behaviour. Thus, this work provides an objective foundation to assist development, evaluation and refinement of conceptual models of ecosystems in this region.

The classes identified here provide a spatial and temporal context within which to interpret existing and future field data. A diversity of ecological data has been collected over considerable periods and large areas of the South Australian Lake Eyre Basin. Previously, interpreting these data as part of a larger whole was hampered by lack of a spatiotemporal context. This work begins to provide a framework within which to consider how these different ecological field records may be combined to further improve our understanding of LEB systems. Furthermore, this work provides an objective geographic stratification which could guide the location and timing of future field ecological sampling effort and hence improve its effectiveness and efficiency. Conversely, comparing the classes identified here to existing vegetation community mapping (e.g., the IBRA) may provide insight into whether differences in vegetation composition coincide with differences in temporal greenness pattern.

In addition, there is scope to examine the temporal profiles of key areas (individual pixels, (250 x 250 m), or small regions (a few square kilometres), as opposed to the regional temporal profiles (thousands to tens of thousands of square kilometres), to provide detailed spatiotemporal greenness and inundation information. This could provide continual historic context for sites with sporadic sampling, or gaps in sampling.

Furthermore, expanding this analysis to the entire Lake Eyre Basin would provide a better understanding of the landscape scale spatiotemporal vegetation behaviour of the region as a whole, including the north-eastern catchments of the Georgina, Diamantina and Cooper. Additionally, an examination of long term trends in greenness and breaks in those trends, in conjunction with climatic information over the whole Lake Eyre Basin should better identify the weather systems which impact the different river systems. This will facilitate understanding of which rainfall events are likely to result in inundation in particular river systems, and begin to predict timing and geography of connectivity of riparian biological communities within and between these systems. In addition, this broader temporal climatic understanding of the region will assist in understanding the consequences of climate change impacts.

Finally, the temporal greenness patterns for the classes identified here were compared to rainfall for the same area. This was used as an indicator for whether a class was dryland or riparian. A class was considered to be dryland if much of the observed temporal greenness signal corresponded with the local rainfall, and riparian if the temporal greenness profile displayed significant variation not-corresponding to local rainfall. A more proximal, and more relevant comparison would be to link the greenness data for riparian classes to river gauging station records. This would allow examination of correspondence between riparian temporal greenness, and one of the proximal drivers of greenness (inundation). Additionally, it might be informative to compare temporal greenness to temperature, which is another major driver of vegetation greenness.

3. Detecting and mapping vegetation indicators of groundwater dependent ecosystems

3.1 Introduction

This component of the report investigates a stretch of Arckaringa Creek to conduct a localised spatial analysis of vegetation within the creek channels and adjacent areas to develop indicators of ecological condition. The presence of perennial trees in riparian ecosystems in the Lake Eyre Basin is generally considered an indicator of long-term sustained, although often intermittent, riverine flows or of access to groundwater. However, the distribution of dominant riverine trees (*Eucalyptus* and *Acacia* species) in the river systems of the LEB is not well documented beyond anecdotal information and a very limited number of biological survey locations. This study sought to detect and map the distribution of these indicator tree species using potential differences in their spectral reflectance characteristics as recorded *in-situ* and in airborne hyperspectral imagery. Such differences have been used to discriminate and map wetland vegetation species associated with springs in the LEB (White et al. 2013), southern Australian arid vegetation species (Lewis 2000, Lewis et al. 2001) and at other arid locations in Australia (Youngentob et al., 2011) and North America (Thorp et al., 2013), suggesting that detection and mapping of these arid riverine trees might be possible. Consequently the aims of this study were to:

- Determine a methodological approach using hyperspectral imagery to detect and map indicator vegetation species (perennial evergreen acacia and Coolabah) to develop long-term ecological measures of riparian vegetation health; and
- Evaluate the potential to detect and map *Eucalyptus coolabah* using hyperspectral image pixel unmixing techniques to determine locations of potential groundwater and surface water persistence.

Spatial indicators of groundwater dependent ecosystems (GDEs) and riparian vegetation health were developed using remotely sensed hyperspectral airborne imagery. The imagery was analysed using an image pixel spectral unmixing approach to detect vegetation species associated with GDEs and surface water permanency. An additional line of evidence from previous hyperspectral analyses which spatially maps a sensitive indicator of vegetation health (the red-edge position) was used to draw comparisons with the mapped fractional covers of the spectral unmixing analyses.

3.2 Study site

Arckaringa Creek was selected as the study site for development of ecological indicators of condition. The creek is located within the Lake Eyre Basin (LEB) and forms part of the Neales/Peake Creek catchment (Figure 10). The creek is representative of ephemeral arid rivers within the LEB and is of particular interest because of the potential for future impacts from open cut coal mining and associated dewatering within the creek and its catchment. This scenario provides an excellent context for development of indicator tools for changes in anthropogenic impacts and identification of spatial hotspots of stressors. Arckaringa Creek is relatively pristine, although has localised impacts from cattle pugging and grazing.

A baseline study of Arckaringa Creek conducted between 2013 and 2014 (White et al., 2014), identified a number of indicator perennial vegetation species. It has been suggested that *Eucalyptus coolabah* is associated with surface water persistence and groundwater permanency, and in particular may be an indicator of the presence of GDEs within the creek (T. Gotch, *pers. comm.*) The tree species *Acacia cambagei* (Gidgee), *Acacia salicina* (Broughton willow), *Acacia estrophiolata* (Ironwood), *Acacia stenophylla* (River cooba) are characteristic of riverine vegetation along the creek and are considered useful indicators of the long-term condition of the creek. The presence and vigour of these tree species could be used to indicate the status of flows and groundwater status in the creek. They occur in mixed stands, their composition varying along the creek. *Acacia cambagei* is more prevalent from Arckaringa station within the upstream reaches to the edge of Mt. Barry/Nilpena stations. Tree stands transition to mixed stands with *Acacia salicina* predominant from Nilpena station to the lower reaches, where Arckaringa Creek confluences with Peake Creek. Understorey grasses, herbs and forbs were relatively abundant in February 2014 in response to recent rainfalls (Arckaringa station recorded 25 mm and 50 mm of rain on 1st and 14th February 2014, respectively; and Mt. Barry station recorded 10 mm and 60 mm of rain on the same dates – *pers comm.* Jackie Williams, February 2014). At least three grass species were present along the creek, including Mitchell Barley grass (*Astrebla* spp.) and Buffel grass (*Cenchrus ciliaris*) (refer to DEWNR report, 2014, for further details).

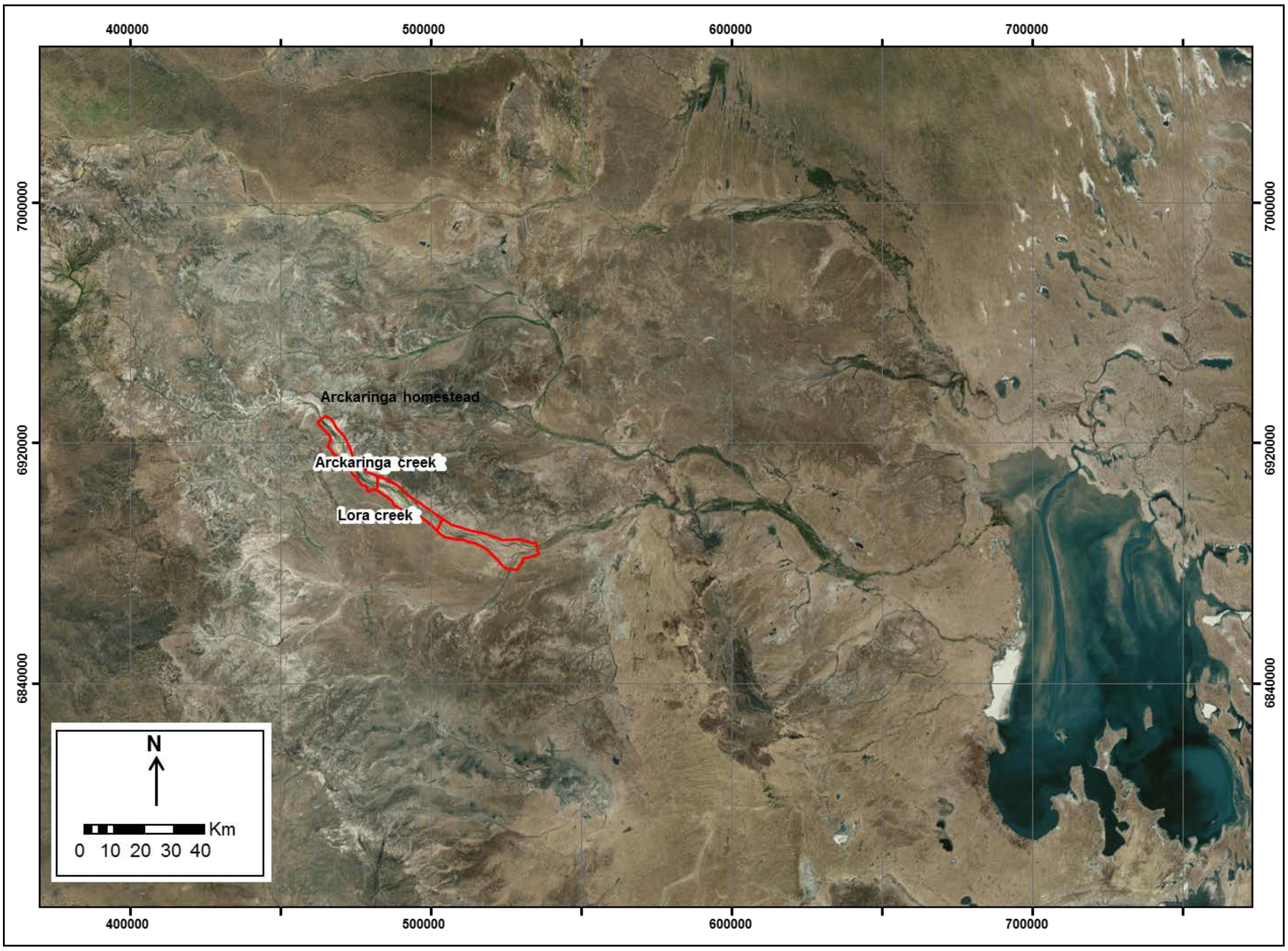

Figure 10. Location of study area on Arckaringa Creek, South Australia. The red boundary indicates the extent of the HyMap hyperspectral airborne imagery capture.

3.3 Methods

Most methods for hyperspectral image-based mapping of vegetation compare reference signatures of plants with image spectral information, using a diversity of algorithms. Many of these involve image 'unmixing', that is, identifying the relative contribution of several ground cover components to the mixed pixel spectra in the image. For this study the reference signatures were derived from field spectroscopic measurements and the hyperspectral imagery, while two approaches to image unmixing were evaluated for detection and mapping the riverine tree species, as described below.

3.3.1 Data

The primary image data used was HyMap airborne hyperspectral imagery consisting of numerous, near contiguous wavebands. The imagery was captured in the first week of March 2014 for the DEWNR Arckaringa Creek project (White et al., 2014). The imagery comprises 126 wavebands with a wavelength range of 450 -2,500 *nm* (Kruse et al., 2009; Cocks et al., 1998), with 3 m spatial resolution (pixel size) and swath width (that the sensor captures as it flies overhead) of 1.5 km. The HyMap imagery was provided pre-processed by HyVista Corporation and includes an atmospheric correction with the HyCorr atmospheric correction model[1], geometric correction and colour balancing of swaths (flight lines the sensor captures) to form a seamless mosaic. The resulting imagery comprises scaled pixel values of apparent surface reflectance that can be compared with reflectance signatures measured on the ground.

On-ground field data were also recorded during two botanical surveys conducted on 29th April – 7th May 2013 and 25th – 26th February 2014 (the latter undertaken near concurrently with airborne hyperspectral image capture) during the DEWNR baseline study. Table 2 provides a summary of this field data.

Table 2. Summary of botanical survey data recorded for Arckaringa Creek, South Australia

		April/May 2013 survey	February 2014 survey
On-ground data recorded	Vegetation cover	✓	✓
	Vegetation species composition	✓	✓
	Site and plot photographs	✓	✓
	DGPS plot locations	✓	Same locations as 2013 survey
	Voucher specimen collection	✓	
	Spectral reflectance signatures	✓	

Botanical survey data were collected at 52, 9 x 9 metre plots in April 2013, which were positionally located to high precision using DGPS. Survey plots were selected to capture the diversity of riparian, GDE, floodplain and dryland vegetation communities within the creek and surrounding landscape. Records included vegetation cover, species composition, and identification of indicator perennial species and understorey. Photographs of the vegetation and substrate were collected to assist with image analysis and interpretation. The second field botanical survey undertaken in February 2014 revisited 13 of the previous botanical survey plots located within the north western portion of Arckaringa creek to determine changes in vegetation greenness and cover since the previous survey (White et al., 2014).

[1] http://www.hyvista.com/wp_11/wp-content/uploads/2011/02/hvc_data_products.pdf

The rainfall just prior to the February 2014 survey led to a greening-up of the creek riverine and floodplain vegetation along with new growth of ephemeral understorey vegetation. Pools of water also persisted in sporadic localised pools along the creek channels. This greener vegetation growth contrasted with the drier conditions under which the April/May 2013 botanical survey was conducted (Figure 11). The greening understorey vegetation was notable in the on-ground estimates of photosynthetic vegetation cover which were markedly higher in February 2014 (White et al., 2014).

(a) (b)

Figure 11. Greening of vegetation understorey between botanical surveys in: (a) April/May 2013; and (b) February 2014

Detailed spectral signatures of indicator vegetation species were recorded with a field spectroradiometer (ASD FieldSpec Pro; 350-2500 nm) to inform the hyperspectral image analyses (White et al., 2014). Reflectance signatures were recorded for indicator species (perennial trees – Acacias and Coolabah), understorey (grasses, herbs and forbs) and their associated variability. A range of pure spectral signatures were recorded in order to capture the main contributions to variability in the plants of interest: dry (non-photosynthetic) tissue, including leaves, bark and ground litter, and green (vigorous/healthy) foliage. The variability in the plants is represented as differences in the spectral signatures, including overall reflectance (brightness or albedo), as well as differences in water absorption and reflectance features at specific wavelengths.

3.3.2 Spectral pre-processing

The reference spectra from field spectrometry measurements were supplemented with pure spectral signatures derived from the imagery. These were selected by overlaying the DGPS points of the botanical survey plots with a false colour composite of the hyperspectral imagery. Regions of interest of known pure pixels of each vegetation type of interest were then created in the image processing software using heads-up digitizing.

The spectral reflectance signatures of the indicator plants from field spectrometry and the imagery were pre-processed and evaluated to determine the nature and quality of the spectra, as well as select optimal spectra for the image analysis. The pre-processing used VIPER tools software (Roberts et al., 2007): the steps are summarised in Appendix 2. This evaluation determined which eamples within a group of spectra (in this case vegetation type) were most representative of their class while covering the range of variability within the class (Roberts et al., 2007). The selected spectra, which are known as endmembers, were pure in terms of their representation of the materials on the ground, in the case of this study different components and expressions of the vegetation types. Plots of the optimal image-based and field reference pure spectral signatures are presented in Appendix 3.

3.3.3 Image analysis

The analysis of the hyperspectral imagery employed two algorithms to detect and map the distribution of indicator species in the HyMap imagery: Spectral Mixture Analysis (SMA) and Multiple Endmember Spectral Mixture Analysis (MESMA). Both were implemented with VIPER tools specialist proprietary software as a plug-in for ENVI image processing software (Roberts et al., 1998; 2007; Dennison and Roberts, 2003; Dennison et al., 2003; 2004)[2].

SMA is based on an assumption of linear mixing of spectral signatures within an image pixel, where the on-ground reflectance of a pixel is determined by the sum of the reflectance of each material within the pixel multiplied by its fractional cover. However, SMA is limited as it allows for only one pure spectral signature per material and does not account for variations present within the same material (Dennison and Roberts, 2003). MESMA models mixed pixels spectrally using linear combinations of several pure spectral signatures, which are allowed to vary in number and type for each image pixel (Dennison and Roberts, 2003). MESMA has the flexibility to use a number of optimal pure spectral signatures for each material/object of interest on the ground, capturing the variability of each material, namely indicator plants for the current study. MESMA enables the mapping of materials on the ground (plants in this instance) and their fraction within the image and its pixels (Dennison and Roberts, 2003).

Initial exploratory image analysis employed SMA to evaluate use of single reference spectral signatures for the indicator plants to identify the same spectral signatures in the hyperspectral image pixels. SMA was conducted for the detection and mapping of Coolabah and acacia (Gidgee and Broughton willow) in the imagery. The results of this approach exhibited some success. The SMA outputs were also used to inform the selection of pure spectral signatures for the MESMA mapping, narrowing down those which were likely to be most successful when used in combination for the MESMA processing.

However MESMA was deemed the most appropriate approach to employ for detecting indicator plant species for several reasons:

- the plants of interest inherently exhibit fractional cover. For example Coolabah have open mixed canopies often exposing the ground cover beneath them;
- mixed cover is common within the 3 m pixels of the imagery. For example different species of acacia are sometimes mixed with Coolabah and understorey plants are often exposed beneath Coolabah canopies; and
- variation within the plants investigated is known to exist from the on-ground botanical surveys. For example single-species stands of Coolabah contain green foliage, woody branches and twigs, bark and dry leaf litter on the ground, all of which contribute to the image pixel spectra of these stands.

A range of optimal endmember combinations which had been selected by the preliminary analysis were input into the MESMA models. The models were run with endmember fractions, error and residual thresholds indicated as optimal by previous studies of Californian chaparral vegetation (Roberts et al. 1998) and semi-arid rangeland vegetation (Thorp et al. 2013) (see Appendix 2). Modifying the constraints improved fraction map outputs for some of the endmember models. The

[2] Available as a freeware, open-source plug-in from the Visualisation and Image Processing for Environmental Research (VIPER) lab at the University of California Santa Barbara and the University of Utah.

combinations of pure spectral signatures (endmembers) used in the MESMA processing and constraints used are summarised for the best model outputs in Table 3.

Table 3. Summary of best endmember models used for the MESMA hyperspectral image analysis

Indicator species modelled	Mixture endmember models	Model constraints	Model performance
Acacia cambagei and *Eucalyptus coolabah*	MESMA two-endmember model: dry and photosynthetic were used for both plants (image spectra)	• Default fractions • No RMSE threshold or residual count • Photometric shade	Poor
Mixed *Acacia cambagei* and *Eucalyptus coolabah*	SMA two-endmember model: mixed photosynthetic Coolabah and *Acacia cambagei*	• Default fractions • No RMSE threshold or residual count • Photometric shade	Corresponded with image false colour composite of riparian vegetation, generally overmapped
Eucalyptus coolabah	MEMSA two-endmember model: photosynthetic Coolabah	• Default fractions • No RMSE threshold or residual count • Coolabah shade spectrum	Generally overmapped
Eucalyptus coolabah	SMA one-endmember model: photosynthetic Coolabah (field spectra)	• Default fractions • No RMSE threshold or residual count • Coolabah shade spectrum	Corresponded with image false colour composite of riparian vegetation, and some Coolabah plots
Eucalyptus coolabah	MEMSA two-endmember model: photosynthetic Coolabah (image spectra)	• Default fractions • Default RMSE threshold and residual count • Photometric shade	No Coolabah mapped

3.3.3 Evaluation of vegetation mapping

Because many of the vegetation survey plots containing Coolabah and *Acacia* spp. were used to derive 'training' data for the MESMA analysis in the form of *in-situ* or image-derived spectral signatures, there was insufficient independent data to conduct a formal assessment of the accuracy of the mapping. Consequently the evaluations of the mapped distributions provided here are based on subjective interpretation in relation to the riverine vegetation evident in the HyMap imagery as well as location and species composition of the survey plots.

In addition the mapping of indicator species derived from MESMA was compared with image-based indicators of vegetation health produced in previous research conducted as part of the DEWNR study (White et al., 2014). That research investigated the health of the riparian vegetation using red-edge position analysis of the HyMap hyperspectral imagery over Arckaringa Creek. The red-edge position is a sensitive measure of vegetation vigour or health, producing a range of quantitative values which can be associated with health of perennial trees, such as different acacia, and Coolabah which are associated with ground water and surface water persistence. Dawson and Curran's (1998) Lagrangian interpolation technique was used for computing the red-edge position on image reflectance signatures (the point of maximum inflection or slope between chlorophyll absorption in the red part of the electromagnetic spectrum and maximum reflectance in the near-infrared) (White et al., 2014).

3.4 Results and Discussion

Overall, the results of the spectral SMA and MESMA unmixing approaches showed some success in mapping fractions of *Eucalyptus coolabah* and *Acacia cambagei*. However, no single output mapped the indicator vegetation types with complete success in terms of spatial location and coverage throughout the creek. Therefore, the results focus on the more general mapping of mixed *Eucalyptus coolabah* and, in the context of determining the condition of the creek via the health of perennial evergreen trees, and an evaluation of the best *Eucalyptus coolabah* fractional maps.

3.4.1 Detection and mapping of riparian perennial evergreen tree species

A number of iterations of the SMA and MESMA modelling were used in exploring the optimal image and field spectral signatures and differing combinations of these for differing configurations of model constraints, with the best outcomes summarised in Table 3. The best performing image analyses used a SMA two-endmember model with mixed stands of photosynthetic *Acacia cambagei* and *Eucalyptus coolabah* image-derived endmembers (Table 3; Figure 12). The spatial distribution of mixed *Acacia cambagei* and *Eucalyptus coolabah* corresponded well with creek channel locations, visual comparison with the false colour composite hyperspectral imagery and botanical survey plot species compositions, particularly for *Acacia cambagei*, although the vegetation fractions are likely to be overmapped. Fractional maps of *Eucalyptus coolabah* showed sporadic spatial distribution and did not always correspond with the composition of botanical survey plots.

A second line of evidence, maps resulting from red-edge position analysis (Figure 13; White et al., 2014), supported and corroborated the spectral unmixing results which most successful mapped vegetation fractions of *Acacia cambagei* and *Eucalyptus coolabah*. The spatial distribution of the mapped fractions of *Acacia cambagei* and *Eucalyptus coolabah* corresponded well with that of larger shifts in the red-edge position to longer wavelengths, which were associated with greener perennial trees (White et al., 2014).

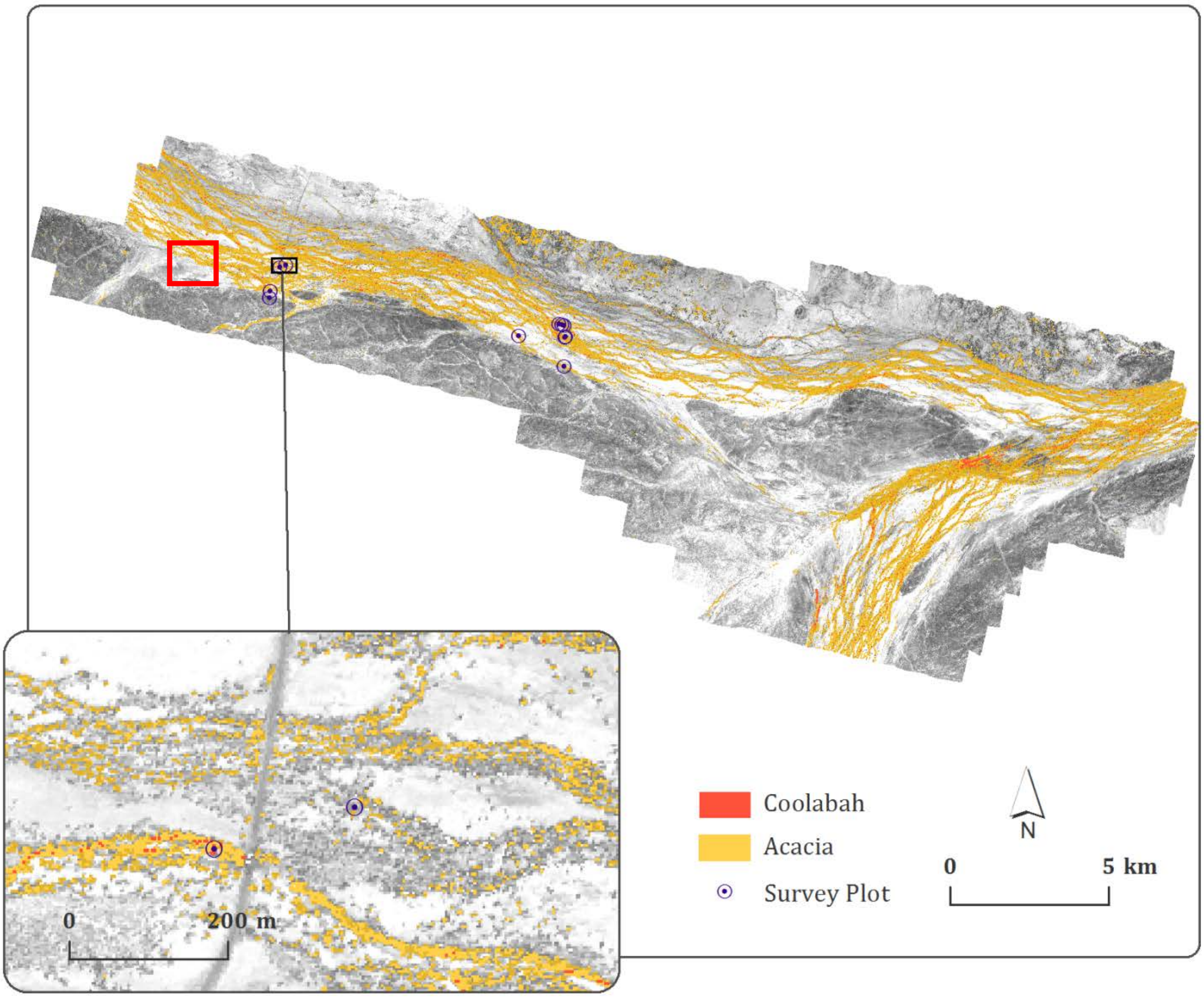

Figure 12. Mapped fractions of *Acacia cambagei* and *Eucalyptus coolabah* along the central portion of Arckaringa creek. The model used was a SMA two-endmember model: mixed photosynthetic *Eucalyptus coolabah* and *Acacia cambagei* (Table 2). Backdrop image is greyscale HyMap image.

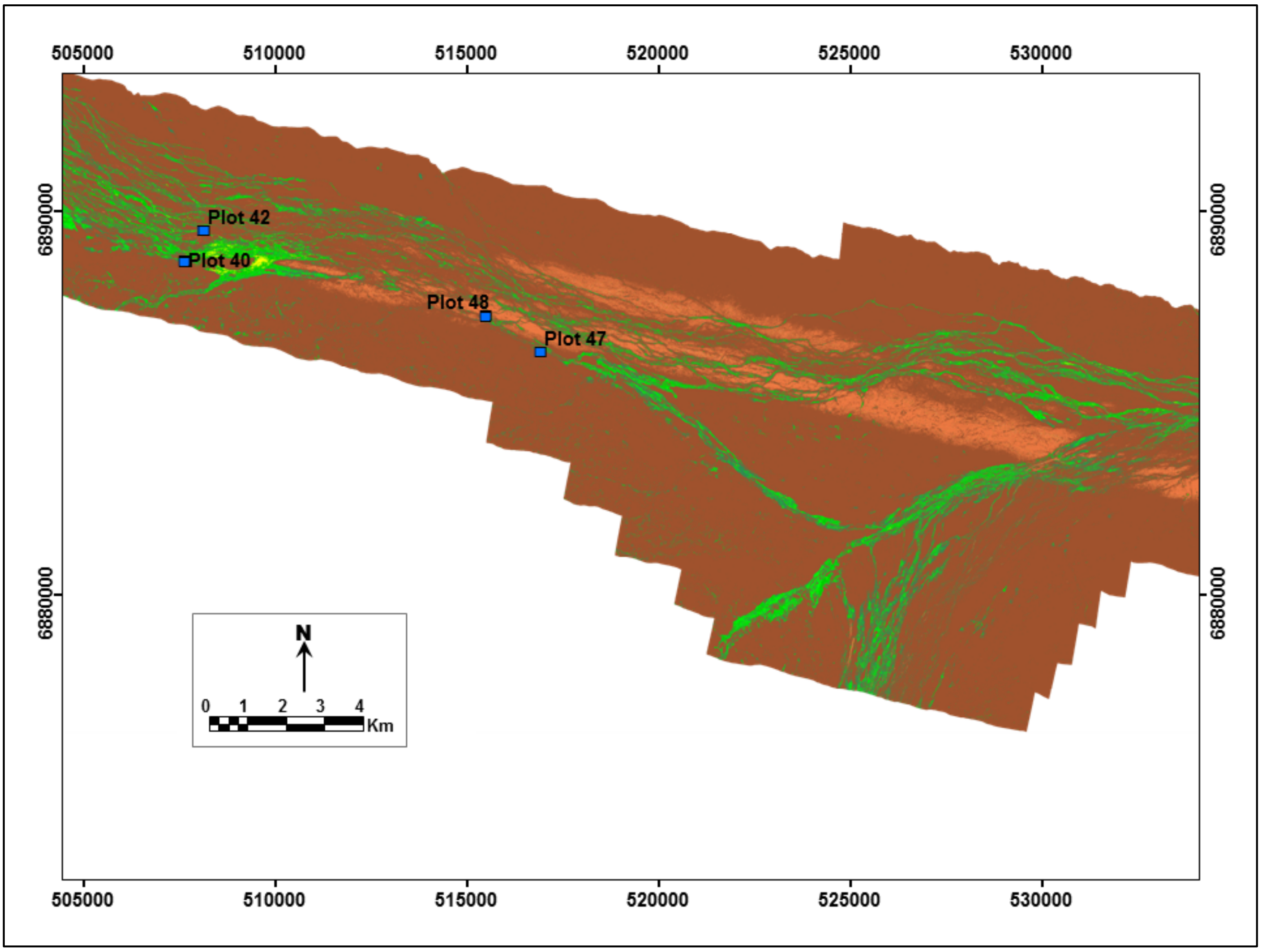

Figure 13. Vegetation health along Arckaringa creek mapped by Lagrangian red-edge position of HyMap hyperspectral imagery (source: White et al., 2014). Colour gradient ranges from sienna associated with shorter wavelength shifts in the red-edge position to, greens, to yellows with a longer positive wavelength shifts in the red-edge position, associated with healthy vigorous vegetation with more complete on-ground cover.

3.4.2 Detection and mapping *Eucalyptus coolabah*

The mapping of *Eucalyptus coolabah* was more challenging due to the nature of the canopy, open and above the acacia canopy, and location of the trees adjacent to creek channels where surface water can persist and understorey varies (dry leaf litter, green forbs and grasses as well as varying soils). The best performing unmixing model for *Eucalyptus coolabah* used a SMA one-endmember model using field reference spectra (Table 3; Figure 14). The mapped distribution of the *Eucalyptus coolabah* corresponded with expected occurrence, based on visual assessments during the botanical surveys, although mapped fractions did not always correspond with botanical survey plots where *Eucalyptus coolabah* was recorded. Overall, *Eucalyptus coolabah* was present along creek channels where surface water is most persistent, and also corresponded with some field observations of *Eucalyptus coolabah* along the main flow channels of the creek. A positive spatial association of the location of *Eucalyptus coolabah* fractions with the red-edge position outputs suggests that the MESMA approach has mapped the densest and most vigorously growing canopies. Shifts in the red-edge position to longer wavelengths were found to correspond with where the permanent greener vegetation was present, such as *Eucalyptus coolabah* (Figure 13 & Figure 14).

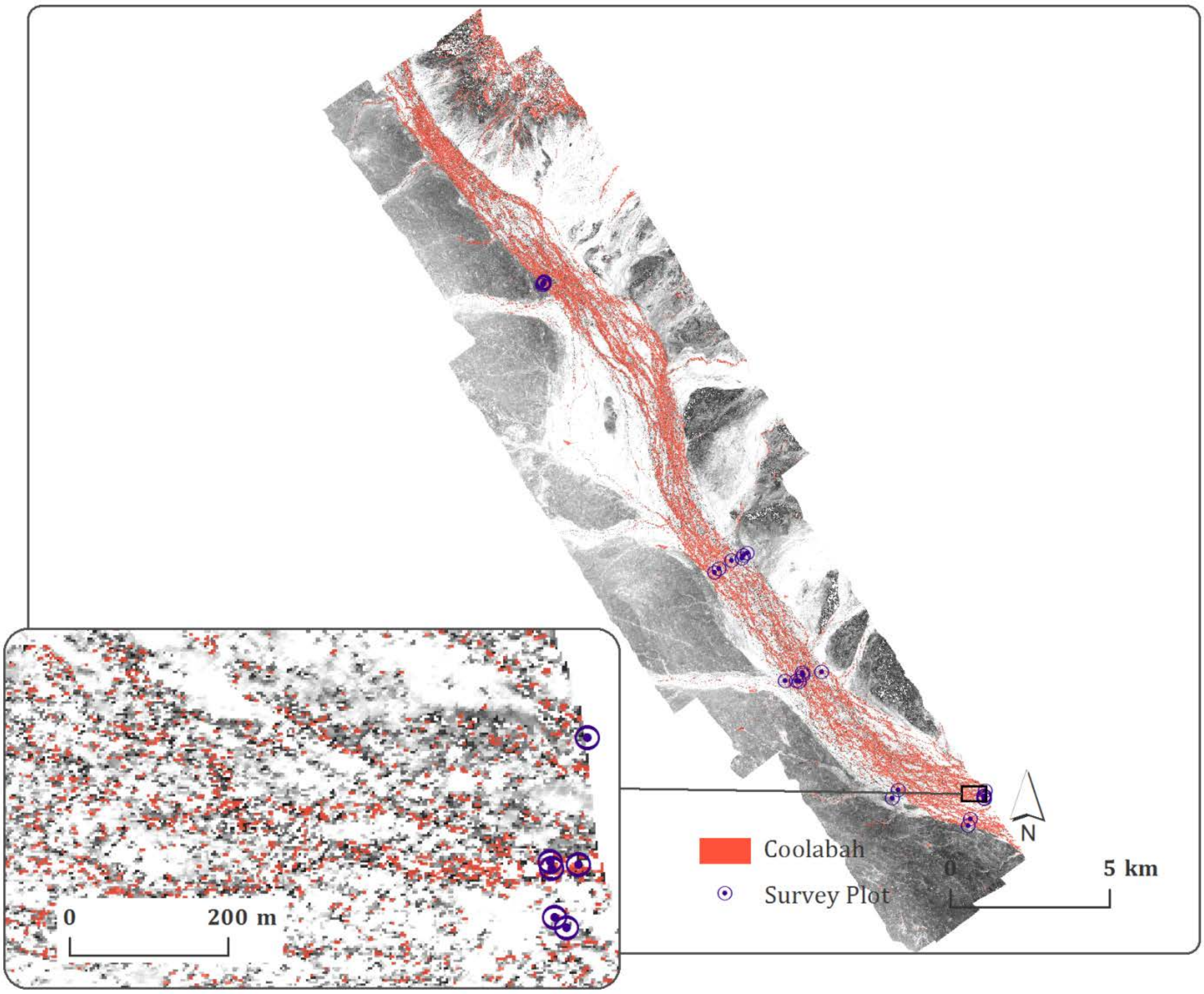

Figure 14. Mapped fractions of *Eucalyptus coolabah* along the central portion of Arckaringa creek. The model used was a MESMA two-endmember model: photosynthetic *Eucalyptus coolabah* (Table 2). Backdrop image is greyscale HyMap image.

3.5 Conclusions and Recommendations

The SMA and MESMA spectral unmixing of the hyperspectral imagery had some success in detecting and mapping indicator species of long-term riparian zone health (mixed perennial evergreen trees – Acacias and *Eucalyptus coolabah*) and potential locations of surface water persistence and near-surface groundwater (*Eucalyptus coolabah*). The SMA mapped outputs, particularly for *Eucalyptus coolabah*, did not always correspond with the on-ground botanical survey observations, although did correspond visually with previously mapped indicators of vegetation health associated with the densest riparian photosynthetic vegetation. Qualitative evaluations suggest that the SMA mapped vegetation fractions for mixed *Acacia cambagei* and *Eucalyptus coolabah* performed quite well although *Acacia cambagei* was overmapped. The mapped *Acacia cambagei* and *Eucalyptus coolabah* corresponded well with the red-edge position outputs, where shifts in the red-edge position associated with healthier more vigorous vegetation corresponded with permanent photosynthetic evergreen trees.

Consequently it appears that the SMA and MESMA unmixing approaches applied to the HyMap hyperspectral imagery have potential for detecting and mapping indicator riparian plants. Both the MESMA mapping of indictor tree species and the red-edge analysis of the hyperspectral imagery appear to detect and map variations in riparian tree crown density and vigour, valuable indicators of ecological conditions, and information which could be used for estimating evapotranspiration within the river catchments. However, the discrimination of different tree species within the riparian vegetation may be limited at the 3 m spatial resolution of the airborne HyMap imagery, even if the species have distinctive spectral signatures. The sparse canopies of the trees and their inter-mixed distributions in the riparian zone mean that their reflectances will generally be mixed in the pixels of the imagery, making their discrimination and mapping difficult.

However, the maps of selected riparian tree species presented in this study can be considered as proposed distributions which should be more thoroughly tested with additional independent data. The field samples used in this study (which had been collected for prior research) were too few to provide independent training and validation datasets. Consequently a formal assessment of the accuracy of the maps has not been possible within the present study, but should be conducted before firmer conclusions about the success of this hyperspectral mapping approach can be drawn. More comprehensive data for validation could come from further field surveys of vegetation composition, or from visual interpretation of high-resolution imagery, if the latter permits discrimination of dominant trees.

With wider application and further ground validation there is also scope to integrate the ecological indicators of arid ephemeral creek condition derived from hyperspectral image analyses with other data to develop indicators of ecological condition for LEB rivers. For example, the mapping of vegetation ecological indicator species developed in this study could be compared with ancillary on-ground data that has been collected during other environmental studies in the Arckaringa Creek catchment. These include logger streamflow and sap flow data at sites where the indicator species are present and stem diameter and trunk spacing data that has been recorded at selected western river waterholes by DEWNR. These data have been recorded at selected sites along Arckaringa creek and adjacent, interconnecting creeks, at time intervals that coincide with the hyperspectral image capture and botanical surveys. Relationships between the locations of indicator species, mapped vegetation health/vigour, stem diameter and trunk spacing and sap flow measurements and streamflow data could be investigated.

In addition, a deeper understanding of the climatic and hydrological drivers of the riparian vegetation could be gained by relating the health and vigour of *Eucalyptus coolabah* and *Acacia cambagei* as mapped by the studies reported in this section to the distribution and frequency of inundation derived from Water from Space (WOfS) analysis (Section 5).

4. Relating landscape processes with gene flow in fish species

4.1 Introduction

Understanding the relationships between population connectivity (i.e. dispersal or gene flow) and landscape processes is necessary for effective environmental and conservation management. Mapping genetic similarity across a landscape can shed light upon how populations are related by geographic and ecological processes and highlight habitats and environmental factors (e.g. barriers to dispersal) influencing population connectivity. This study attempts to identify the effect of inundation on the genetic differences and similarities of fish sampled across the study area using spatially explicit visualisations and analysis tools.

4.2 Methods

4.2.1 Overview

The broad aim of this study was to demonstrate analyses and applications of new spatial data products to help relate environmental processes to biotic connectivity in the LEB. We developed indicators of hydrologic function from remote sensing and GIS analyses for comparison with results on population genomics of the Golden Perch (*Macquaria ambigua*) detailed in Behregaray and Attard (2015). That work, part of sub-project Task 5: *"Developing a Genomic Approach for Environmental Condition Indicators in the Lake Eyre Basin"*, generated results that provide an opportunity to understand how the hydrologic regime of the Lake Eyre Basin impacts on genetic connectivity of the largest fish species in the region. We a) visualised the genetic similarity across the LEB sub-catchments inferred in Task 5; b) mapped riverine flow paths using a satellite remote sensing-derived measure of inundation to evaluate barriers to the dispersal of fish; and c) compared characteristics of landscape function with genetic similarity using the temporal greenness classes described in Section 2 to explore relationships between landscape processes and genetic similarity.

4.2.2 Data

Eigenvectors of the first function from the Golden Perch discriminant analysis described in Behregaray and Attard (2015) were provided accompanied with geographic coordinates of the original sample locations. The mean Eigenvectors were computed from each individual for each location. The population genomic data comprised 225 individual Golden Perch collected from 14 sampling sites across the LEB. A total of 29,008 DNA markers were genotyped for all fish and from those a selection of 5,649 DNA high quality DNA markers were used for genomic analyses (details in Behregaray and Attard (2015)).

Released in late 2014, Geoscience Australia's "Water Observations from Space" (WOfS) is the world's first continent-scale product of the presence of surface water derived from Landsat satellite imagery. WOfS covers the entire Australian continent at 25 metre spatial resolution, providing information through time-series analysis (1987 to present) on where water is usually seen, such as in lakes and rivers, and where it is unusual, such as during flooding events (Geoscience Australia 2014). Historical surface water observations are derived from the Australia-wide archive of Landsat 5 imagery from 1987 to 2011, and Landsat 7 imagery from 2000 to present. With a revisit rate of 16 days (23 times per year) and some observations affected by cloud, shadow or other quality issues, not all historical floods will have been observed by satellite. The algorithm (LC25-Water) developed for WOfS is designed to locate large areas of water and as a result it may miss small water bodies (Geoscience Australia 2014).

The algorithm developed by Mueller *et al.* (Publication in prep.) used to detect water from each observed pixel is based on a statistical regression tree analysis of a set of normalised difference indices and corrected band values. The regression is based on a set of water and non-water samples created by visual interpretation of 20 Landsat scenes from across Australia (Geoscience Australia 2014).

The final Water Observations from Space (WOfS) product combines all water observations from the entire WOFL time series. There are five summary composite datasets for all of Australia which are publically available online in map form through the Australian Flood Risk Information Portal[3]. These are known as WOfS Summaries (one summary file (25 m resolution GeoTiff) per cell (1 degree x 1 degree tile stack) per dataset, in Geographic Coordinate System WGS 1984).

Data and methods used in producing the temporal greenness classes are detailed in Section 2 of this report.

4.2.3 Analyses

Preparation and visualisation of Golden Perch data

The mean eigenvector from the first principal component of genetic distances was calculated and associated with the fish sample locations. The data was visualised as a map showing the genetic differences between the 14 sampling sites. Using these mean eigenvector outputs is appropriate since these results are consistent with several other analyses of population genetic differentiation in Golden Perch (i.e. other statistics would also produce the same pattern of genetic discrimination in the LEB; details in Behregaray & Attard (2015)).

Mapping flow paths between sample sites using WOfS

The WOfS dataset maps the frequency of inundation for a 25 year period (1987 – 2011). The data were used as a surface to find the most likely path for fish to travel. In this case, a subset of points was selected to serve as a source and destinations. Using a least cost path-finding algorithm, the paths were found from the Neales sample site to Georgina, Diamantina and Cooper sampling sites that were approximately equal Euclidian distances from the source.

The least cost path algorithm (ESRI 2010) requires a raster that defines values that represent 'costs' to traverse each cell. Lower values represent lower costs. The algorithm attempts to find a path across the surface with the least cumulative cost. The WOfS dataset contains values of 0 to 100 representing frequency of inundation for the 1987 – 2011 period. The data was for locations with observed flooding inverted to represent high frequency of inundation as 'low cost' values ranging from 1 – 100,001; where 1 represented 100% inundation frequency, and 100 represented 1% inundation frequency. Cells with 0% inundation frequency were attributed with an artificially high cost value of 100,001 to coerce the algorithm to only traverse the shortest distances across cells with no inundation detected.

The resulting paths (kept as rasters) were used to extract the actual frequency of inundation from the uninverted WOfS data to visualise the hydrologic landscape the path traverses. Areas of low and high frequency of inundation were highlighted in the visualisations.

[3] http://www.ga.gov.au/scientific-topics/hazards/flood/afrip

Relating temporal greenness classes to genetic similarity

The temporal greenness classes provide insight into the different dynamics that drive landscapes in the Lake Eyre Basin. The temporal patterns associated with vegetation greenness and inundation regimes may shape habitat characteristics for aquatic life that may be expressed by their genetic differences and patterns of connectivity. In this section we explore the potential similarities between landscape processes and genetic distances between Golden Perch populations. Six of the Golden Perch sample sites are located within the South Australian Lake Eyre Basin temporal greenness classification study area (Section 2 of this report). We identify the classes within which the sample sites lie, and for each sample site compare metrics of class similarity with metrics of genetic similarity.

The ISOCLASS classification algorithm clustered all pixels in MODIS NDVI time series on the basis of similarity between their temporal profiles. The similarities and progressive grouping of classes are mapped using a dendrogram (Figure 1). The distances between temporal greenness classes that were attributed to the fish sample sites were compared to the corresponding differences between the mean genetic distance Eigenvectors for those sites.

4.3 Results

Two distinct spatial clusters of genetically similar Golden Perch are evident in the region (Behregaray and Attard 2015; Figure 15). Golden Perch from western catchments (the Neales, Warburton, Diamantina and Georgina Rivers) share a strong genetic similarity. Golden perch from eastern catchments (Cooper, Thomson and Barcoo Rivers) are genetically different from those in the western catchments. Thus, a marked genetic distinction between western and eastern LEB populations is evident; i.e. all individual fish sampled in western rivers are likely to have hatched in that region – and vice-versa.

As shown in Figure 17, the least cost path analyses from site 3 to sites 2, 6 and 13, produced a path from site 3 to Lake Eyre where it split to lead to the Cooper Creek catchment for site 13, and split in the Diamantina River catchment near the Georgina River catchment to lead to sites 6 and 2, respectively. The least cost paths generally follow the streams mapped in the national GIS data, but straight lines are evident in broad floodplains with braided flow channels.

The centre enlargement panel (Figure 16) identifies a potential hydrological barrier for genetic connectivity between the source and site 13 (i.e. between western and eastern catchments). The right enlargement panel identifies a potentially critically important location along the Diamantina that may be necessary for the persistence of fish between the source and destination of site 6.

The temporal greenness classes within which the sample sites fall are shown in Figure 17. The classes surrounding the sample locations are included as the coordinates are known to be estimates (Figure 17). Additionally, instead of the discrete boundaries presented by the classes, the landscape processes function along gradients, and riparian zones are expected to drive water hole function more than the surrounding arid rangelands. Subsequent results are based on the assumption that the sites are within the closest riparian classes, rather than the nearby rangeland classes.

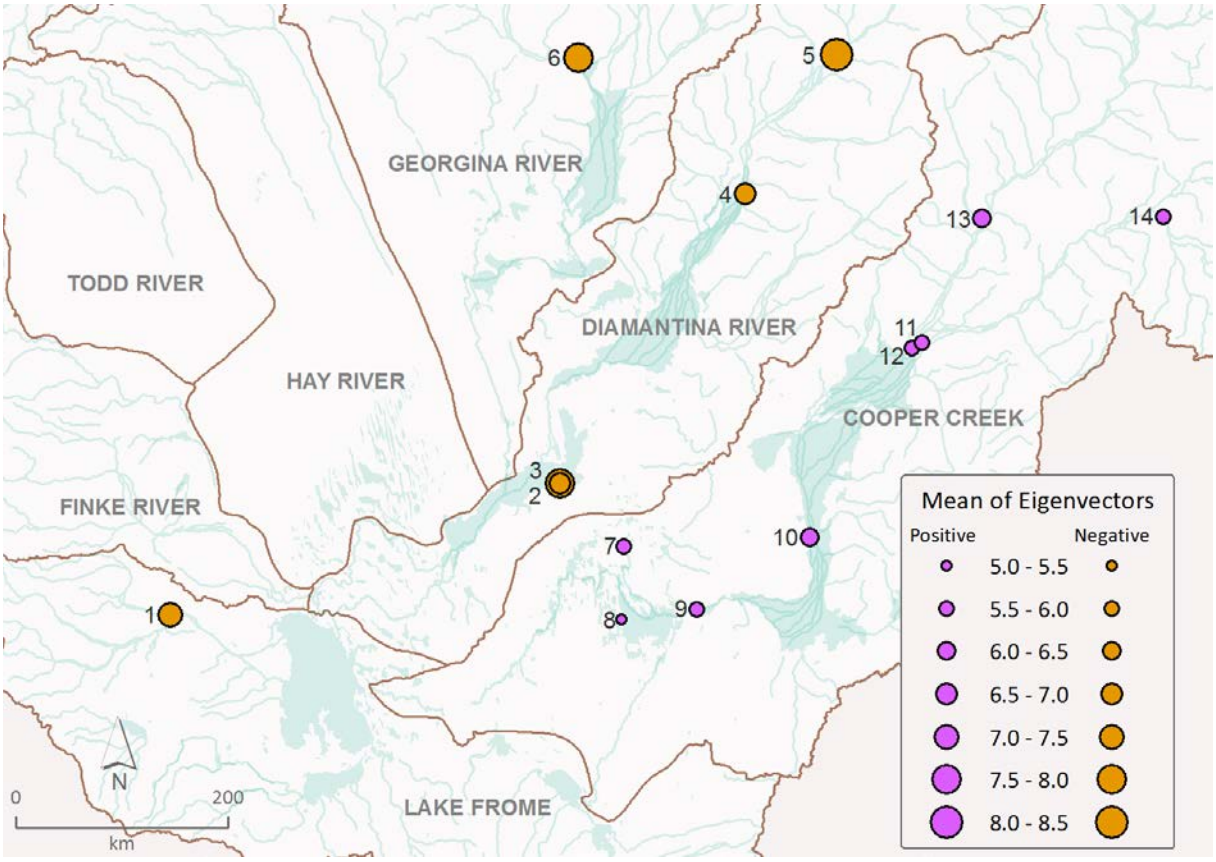

Figure 15. Mean Eigenvectors for Golden Perch sample sites. The size of circles represents the absolute value of the site mean eigenvectors.

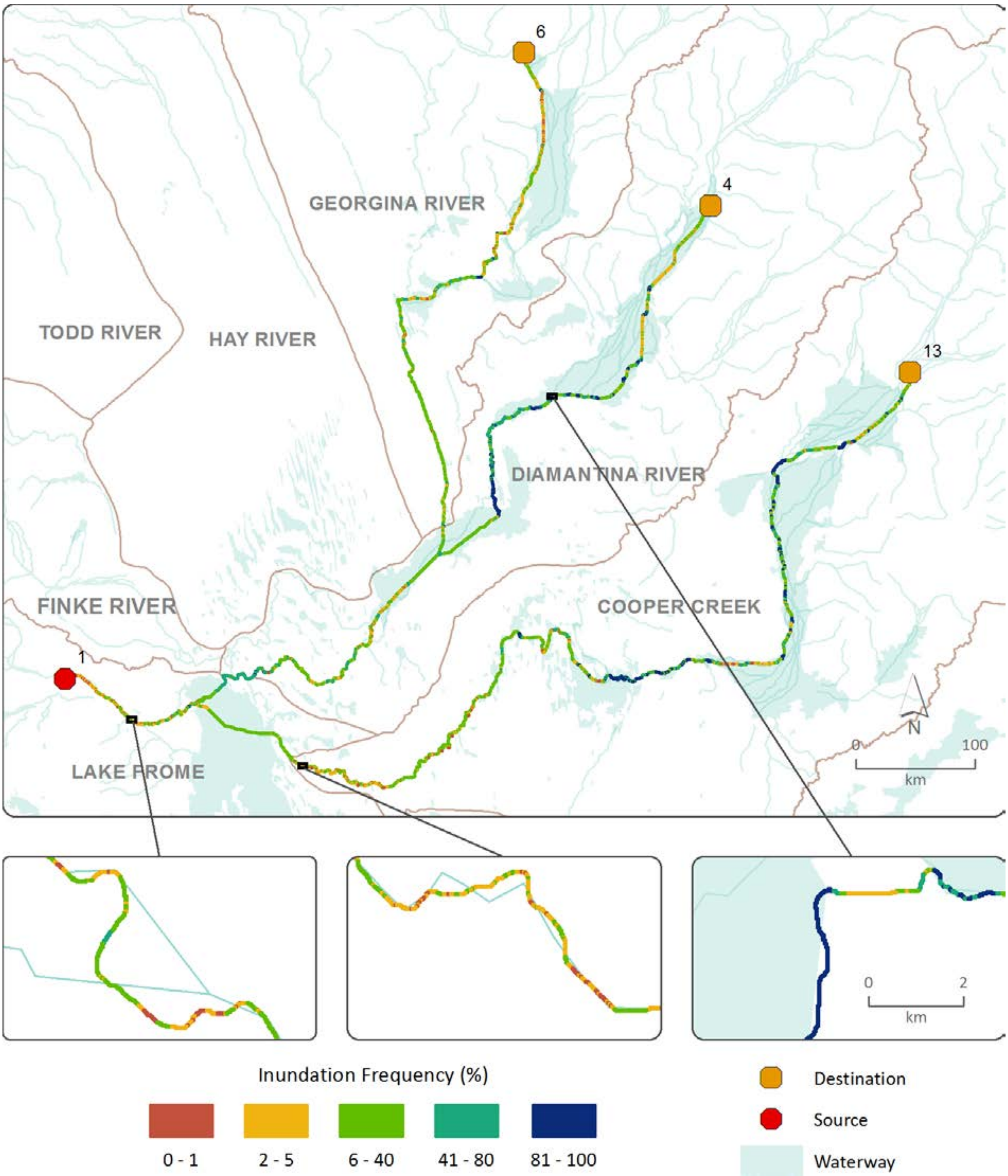

Figure 16. Least cost path analysis using WOfS data; enlargement panels identify segments of the path with medium, low and high inundation frequencies. Underlying waterway data from Geoscience Australia (Crossman and Li, 2015).

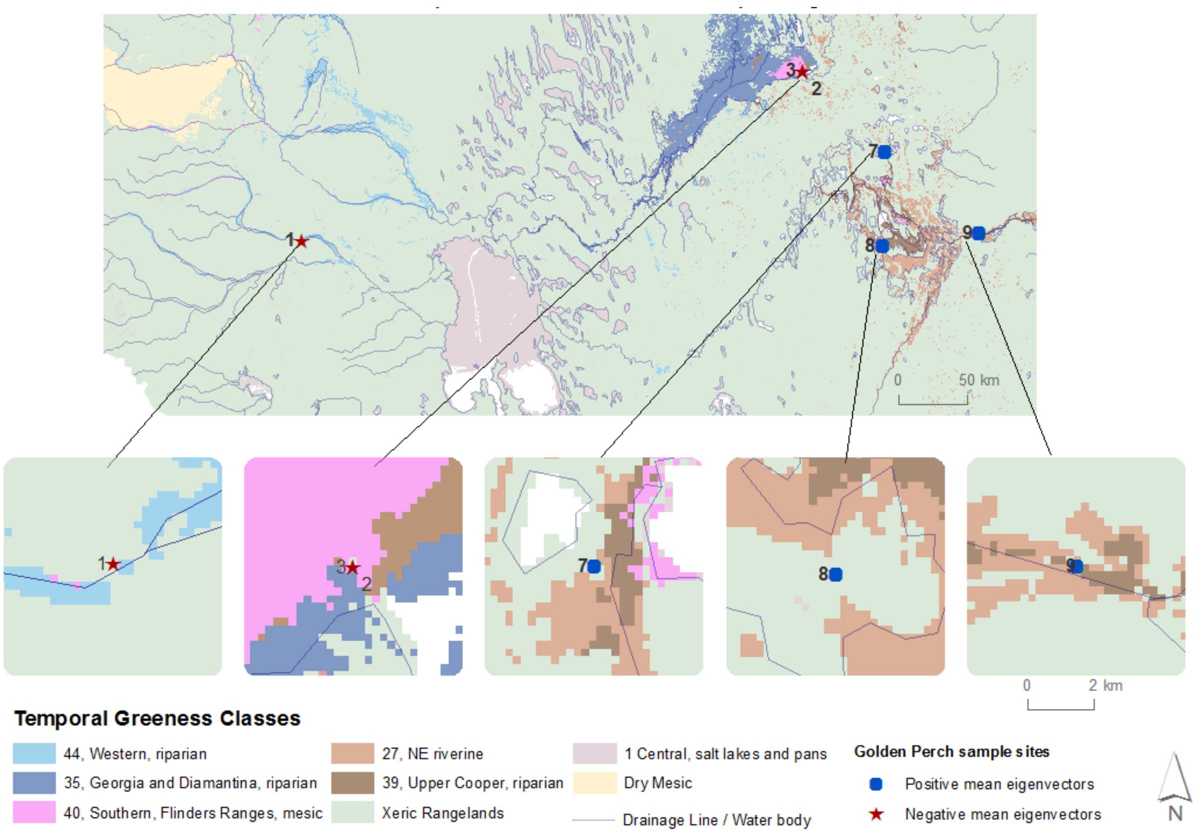

Figure 17. Golden Perch sample sites and the temporal greenness classes within which they occur.

Table 4. Temporal greenness classes for Golden Perch sample sites

Site	Class #	Broad class description
1	44	Western, riparian
2 & 3	35	Gerogina and Diamantina, riparian
	40	Southern Flinder Ranges, mesic
7, 8 & 9	27	North East, riverine
	39	Upper Cooper, riparian
	3 & 10	Xeric rangelands

Table 6 indicates that there are two distinct groups of Golden Perch with genetic similarity- sites 1, 2 and 3 (differences of up to 1.1) and sites 7, 8 and 9 (differences of up to 0.5). These two groups are quite distinct from one another (differences between 12.1 and 13.2).

Sites 1, 2 and 3 fall in or near temporal greenness classes 35, 40 and 44 (Table 4). These classes exhibit relatively low separation of between 5.7 and 6.1 (Table 6). They are most dissimilar to classes 27 and 39 where sites 7, 8 & 9 are located (8.5). Classes 27 and 39 are more similar to one another (6.6) than any of the other classes (8.5).

Table 5. Crosstabulation of differences between sample site Eigenvectors means for Golden Perch (blue and orange numbers highlight genetic similarity between sites).

Site	1	2	3	7	8	9
1	-	0.3	-0.7	-13.2	-12.8	-13.3
2	-0.3	-	-1.1	-13.5	-13.1	-13.7
3	0.7	1.1	-	-12.4	-12.1	-12.6
7	13.2	13.5	12.4	-	0.4	-0.2
8	12.8	13.1	12.1	-0.4	-	-0.5
9	13.3	13.7	12.6	0.2	0.5	-

Table 6. Multidimensional Euclidean class distances between golden perch sample site (blue and orange numbers highlight genetic similarity between sites)

Site		1	2 & 3		7, 8 & 9	
	Class	44	35	40	27	39
1	44	-	6.1	5.7	8.5	8.5
2 & 3	35	6.1	-	6.1	8.5	8.5
	40	5.7	6.1		8.5	8.5
7, 8, & 9	27	8.5	8.5	8.5	-	6.6
	39	8.5	8.5	8.5	6.6	-

4.4 Discussion

The analyses demonstrated in this section offer insight into the potential for these recently developed spatial datasets and techniques to elaborate on our understanding of the relationships between landscape processes and biotic connectivity.

The least cost path analyses of inundation frequency from the WOfS observations illustrate a number of applications relevant to fish ecology and genetics. It can identify flow paths across catchments likely to be used by Golden Perch, highlight potential key refuge locations where inundation is near-permanent, and 'choke points' between those where inundation is intermittent but necessary to connect them. This mapping may be suitable for the classification of aquatic refugia as 'Ark, Disco and Polo' (McNeil et al. 2014) and identify when and how they are connected to allow fish populations to interbreed.

The WOfS dataset is an aggregated summary product of the WOFLS dataset. The WOFLS dataset contains the individual images of inundation produced using Landsat imagery. WOfS provides frequency of inundation as a percentage from all the available Landsat observations. The disaggregated WOFLS can be used to compute summaries of inundation frequency for particular periods such as seasons, years or longer. Specific periods or years of interest can be identified using the temporal greenness class profiles Section 2 of this task report to inquire how flow paths behave during specific flood events or drought.

The integrated analytical framework demonstrated here combines detailed information about hydrological variation and population genomics to disclose key factors accounting for biodiversity structure and connectivity in the LEB. Assessing spatial and temporal environmental factors influencing biodiversity is crucial for implementing appropriate management practices in the LEB rivers. For instance, Golden Perch require increases in flow volume to stimulate reproductive behaviour, recruitment booms and dispersal (Faulks, Gilligan & Beheregaray 2010).

The comparison between inundation regimes and population genetic differences illustrates the potential for exploring relationships between landscape and hydrological process and biological connectivity. It enables predictions to be developed about the interaction between hydrological variation, management of water resources and species (e.g. fish) persistence over the landscape. It also allows for the identification of key barriers for dispersal (e.g. centre enlargement panel in Figure 16) that account for the lack of population connectivity observed across the LEB. In other words, both historic inundation and genomic approaches consistently indicate that western and eastern rivers are not effectively (i.e. functionally) connected, which is a key finding for water management in the region. The results show promise for analysis which expands the temporal greenness analysis beyond the South Australia to encompass the entire Lake Eyre Basin. Doing so would include dynamics from extremely different systems to the North and East, and would include more sample sites for analysis.

5. Understanding water hole persistence at the end of dry periods

5.1 Introduction

Water holes are essential for the persistence of fish populations in the Lake Eyre Basin. However, their patterns of persistence between periods of extensive inundation that reconnect remnant populations are not well understood. Due to the remote and extensive geography of the Lake Eyre Basin, gaining an overview of the persistence of inundation in fish refugia has been problematic. Conceptual models on how fish populations survive the variable inundation regimes require an understanding of how the water holes behave after inundation, how long they persist, and their status during dry seasons. It remains unclear whether the same water holes persist at the end of dry periods, or whether the patterns are variable, like 'blinking lights', due to variable flow paths across the landscape. It is the aim of this study to explore the potential of a new satellite remote sensing inundation mapping product to document the inundation status of known water holes in the Neales-Peake catchment for end of dry periods.

5.2 Methods

The inundation status at the end of four dry periods was determined at water holes in the Neales-Peake catchment as nominated by the South Australian Research and Development Institute (SARDI). The dry periods were determined using the AWAP rainfall product (Section 2.2.3). The end of dry period was defined as the month preceding significant rainfall to break the dry period. The dates were 09/1999, 06/2005, 09/2007, 06/2008.

The Water Observation Feature Layers (WOFL) is the disaggregated data product for the WOfS frequency of inundation summary. Each of the WOFLs is an Australian Geoscience Data Cube (AGDC) tile showing the water classified from the corresponding Landsat Nadir BRDF-Adjusted Reflectance (NBAR) tile. Each WOFL file contains a single layer of 4000 x 4000 pixels, one byte per pixel. Each pixel is coded as follows:

0: No water in pixel
1: No data (one or more bands) in source NBAR tile
2: No contiguity
4: Sea water
8: Terrain shadow
16: High slope
32: Cloud shadow
64: Cloud
128: Water in pixel

In order to maximise the likelihood of encountering one valid observation (either no water (0) or water (128)), tiles for the two months preceding the dry period breaking rain event were amalgamated. The amalgamation involved searching each pixel in the two month period for water (128) and, if not encountered, the search was continued for a valid observation of no water (0). If neither were found, the pixel was attributed as having no valid observation. No valid observations were usually the result of terrain shadow or due to the Landsat 7 scan line correction error satellite that began in 2003.

The entire dataset is broken into tiles of 1 degree latitude and longitude. The Neales-Peake catchment spans 4 of these tiles, (WGS 1984: 33^{o}S - 34^{o}S latitude, 139^{o}-140^{o} longitude). Each tile was coded as described above. Subsequently the final tiles were mosaicked as a single layer per date period.

Geographic coordinates of 55 known waterhole locations were provided by SARDI. The data were cleaned to homogenise coordinate systems. The coordinates referred to point locations that are meant to serve as markers for sampling and do not represent the extent of water holes, many of which change in extent and location from year to year. Each site was therefore attributed as being inundated if a pixel within 500m was coded as water. Sites corresponding to pixels that were coded as not having a valid satellite observation were coded as not having a valid observation.

Figure 18. SARDI Neales-Peake waterhole fish sampling sites.

5.3 Results

Figure 19 shows Algebuckina water holeas an example of the extent of water detected by WOFS for the four dates and its relationship to the SARDI location markers. Considerable variability is evident between the extent of inundation in the four years. The least inundation detected was in September 1999 (900m^2), while September 2002 had the most extensive inundation (65,500 m^2) of the four dates. Algebuckina Midstream and East are the only two that were attributed as being within 500 m of inundation for September 1999. Algebuckina Causeway was only attributed with inundated status in September 1999 and June 2008, along with the other two sites. It should be noted that Algebuckina is the longest and widest of the waterholes, thus may not be challenging the method

The full inundation matrix (Table 7) identifies water holes with disparate characteristics for the four periods. Six of the 55 sites retained detectable water during the four end of dry periods. These were also the only ones that were inundated in 1999, other than EFN027. No detectable water was evident for nineteen of the sites for any of the dates. The remainder exhibit varying behaviour, especially for 2002 and 2005, with either one or both inundated.

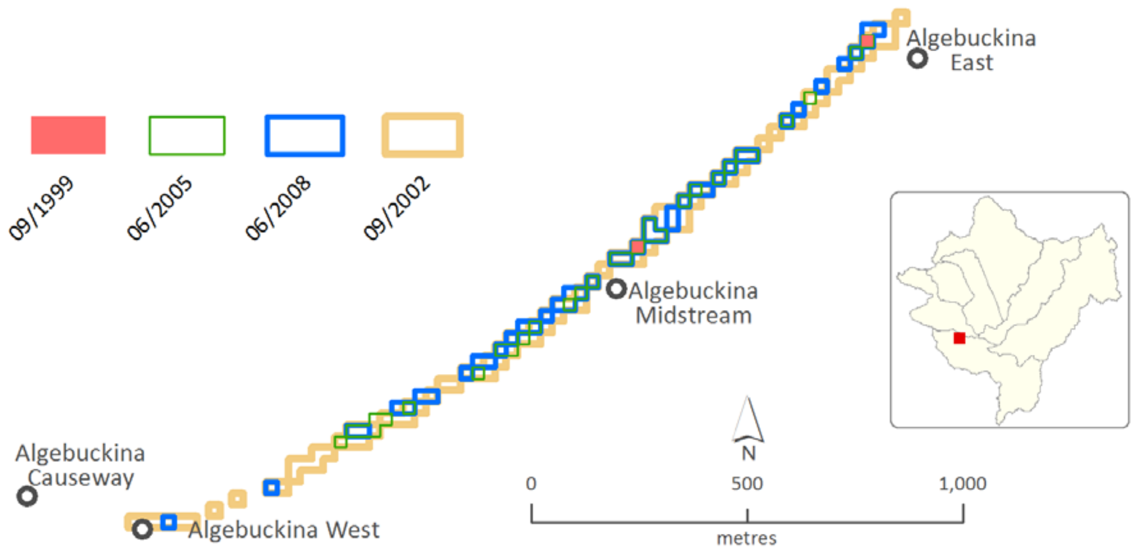

Figure 19. Inundation status for Algebuckina water hole sample sites.

5.4 Discussion

This study demonstrates the capacity for satellites to collect information on remote and far reaching landscapes that are difficult to monitor using traditional methods. Detailing the spatial and temporal patterns of water hole persistence during different climatic conditions can help advance our understanding of how fish persist in waterholes. The full inundation matrix (Table 7) suggests that there are three types of water holes in the Neales-Peake catchment after significant periods of drought: those that are reliably inundated (11% of the waterholes studied that were inundated on all years) , those that are aren't (51%), and the remainder that have variable inundation (38%). The spatial resolution of Landsat (25 m) may be limited for the application of this method for smaller waterholes that are likely to avert detection. Further work is required to validate the accuracy of the results, and may include outputs of the Neales source model for the riverine waterholes. However, the study exhibits the potential of using the AWAP and WOFLs data sets to identify climatic events and map the surface landscape response. Additionally, the different temporal aggregates which can be computed such as frequency of inundation on a seasonal or annual basis can offer insight into the dynamic nature of the Lake Eyre Basin and other hydrologic regimes.

Table 7. Neales-Peake catchment water hole inundation status for four end of dry periods

Site Name	1999	2002	2005	2008
12 Mile Spring	No valid observation	Dry	Dry	Dry
Afghan	Dry	Dry	Dry	Dry
Algebuckina Causeway	Dry	Inundated	Dry	Inundated
Algebuckina East	Inundated	Inundated	Inundated	Inundated
Algebuckina Midstream	Inundated	Inundated	Inundated	Inundated
Algebuckina West	Dry	Inundated	Inundated	Inundated
Andaranna	Dry	Dry	Dry	Dry
Angle Pole	Dry	Dry	Dry	Dry
Arkaringa Creek	Dry	Dry	Dry	Dry
Baltacoodna	Dry	Dry	Dry	Dry
Battersby's Dam	Dry	Dry	Dry	Dry
Big Blythe	Dry	Dry	Dry	Dry
Cramps	Dry	Inundated	Dry	Dry
Eaglehawk Dam	Dry	Inundated	Inundated	Inundated
EFN027	Inundated	Inundated	Inundated	Dry
EFS032	Dry	Dry	Inundated	Dry
Fountain Springs	No valid observation	Dry	Dry	Dry
Freeling Springs 1	Dry	Dry	Inundated	Dry
Freeling Springs 2	Dry	No valid observation	Dry	Dry
Freeling Springs 3	Dry	Dry	Inundated	Dry
Hanns Creek	Dry	Dry	Inundated	Dry
Hawker Springs	No valid observation	Dry	Dry	Dry
Hayley's Dam	Dry	Dry	Dry	Inundated
Hookeys	Dry	Inundated	Dry	Dry
Lora Creek	Dry	Dry	Dry	Dry
Mathieson W/hole	Dry	Inundated	Dry	Dry
Michael Dam	Inundated	Inundated	Inundated	Inundated
Neales Crossing	Dry	Dry	Dry	Dry
Nth Freeling Spr2	Dry	Dry	Inundated	Dry
Nth Freeling Spr	Inundated	Inundated	Inundated	Inundated
Ockenden	Dry	Dry	Dry	Dry
Old Nilpinna	No valid observation	Inundated	Dry	Dry
Old Peake Bore	Dry	Dry	Dry	Dry
One Mile Bore	No valid observation	No valid observation	Dry	Dry
Ood'tta Town Dam	Inundated	Inundated	Inundated	Inundated
Outside Springs 1	No valid observation	Dry	Dry	Dry
Outside Springs 2A	No valid observation	Dry	Dry	Dry
Outside Springs 2B	No valid observation	Dry	Dry	Dry
Outside Springs 3	No valid observation	Dry	Dry	Dry
Peake Crossing	Dry	Dry	Dry	Dry
Road to Cliff	Dry	Dry	Dry	Dry
Road to Tard	Dry	Dry	Dry	Dry
Shepards	Dry	Dry	Dry	Dry
Slate Hole	Dry	Inundated	Inundated	Inundated
South Cliff	Dry	Dry	Dry	Dry
South Stewarts	Dry	Dry	Dry	Dry
Stewarts Waterhole	Dry	Inundated	Dry	Dry
Suspect Dam	Inundated	Inundated	Inundated	Inundated
Tardetakarinna W/hole	Dry	Inundated	Dry	Dry
The Cliff	Dry	Dry	Dry	Dry
Three Sisters Dam	Dry	Inundated	Dry	Dry
U/S Peake	Dry	Dry	Dry	Dry
Warrarawoona W/hole	Dry	Inundated	Inundated	Dry
Winkies	Dry	Inundated	Dry	Dry
Wirriarrina	Dry	Inundated	Dry	Inundated

Key:
- Inundated
- Dry
- No valid observation

6. Mapping and sharing water quality survey data

This component of the project provided spatial data and analysis support for Task 4: *'Nutrient Dynamics and Sources'*. Components included support for a CSIRO field trip to collect water quality data in the Georgina River in September 2014 and subsequent geographic visualisation of the results. The field trip planning included mapping of the distribution of existing water quality records, route and sample site recommendations, training on the use of GPS hardware and software, and advice on data collation for spatial representation.

Water quality information was collected, processed and analysed and is reported in Williams et al. (2015). The results are presented in a website that hosts a keyhole markup file (kmz) for interactive display in Google Earth (Figure 20). The site serves as a pilot demonstration of a format for open data sharing to encourage public interest and to make the information accessible to organisations interested in building upon previous surveys such as these. It is considered desirable to expand the sharing of information such as previous water quality surveys to allow subsequent efforts to develop some temporal, spatial and thematic consistency that are conducive to meaningful analyses.

The URL for the site is https://sites.google.com/site/csirowaterqualitypilot/

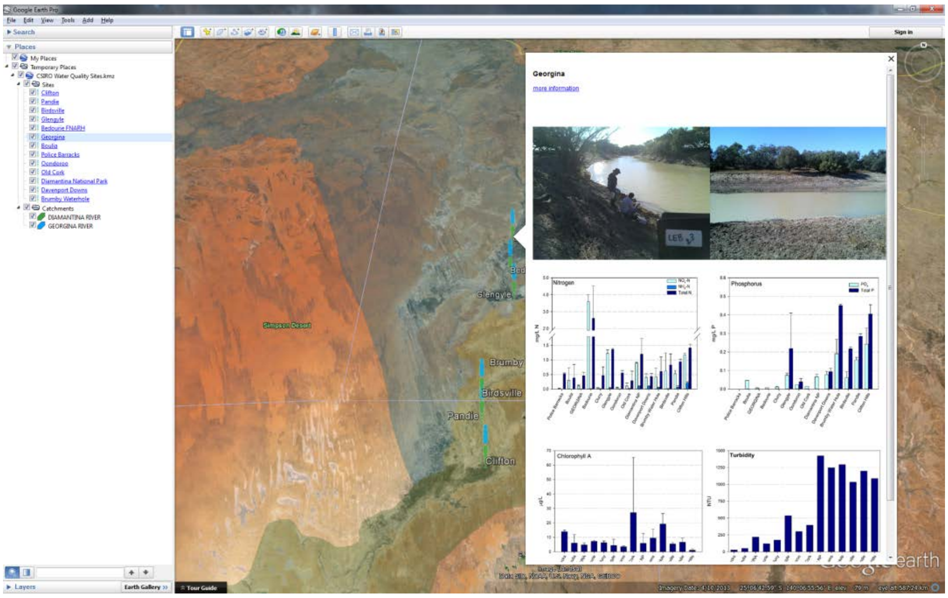

Figure 20. Screenshot of Google Earth kmz of CSIRO water quality parameters for Diamantina Lakes.

7. Conclusions

The research presented in this report has developed and demonstrated new indicators of function and condition for Lake Eyre Basin rivers, drawing on remote sensing, geographic analyses and visualisations.

To date physical and biological sampling in the LEB has been sporadic and sparse, limited by the broad geographic area and difficulty of access as well as logistics and high cost of field studies. While it is known that terrestrial and riverine ecosystems are highly variable across the Basin and over time, traditional sampling and monitoring methods rarely capture the full range of conditions and events. This makes it difficult to reliably compare characteristics of different regions, identify trends over time, differentiate anthropogenic impacts from natural variability and to integrate knowledge about different physical and biological components.

We have used spatially comprehensive satellite image data with long archives of consistent observations of the land surface to provide new understandings of the characteristics and variability of riverine ecosystems in the LEB. We demonstrate that vegetation growth in the rivers in the western part of the Basin differs in magnitude and timing from those of the eastern Basin, being fed by rainfall and flood pulses of different origin (Section 2). In the eastern Basin, the vegetation response of the Georgina and Diamantina Rivers is distinct from that of the Cooper Creek and Coongie Lakes complex, while the Upper Cooper, Cooper flood plain and Coongie Lakes all have different inundation and vegetation greening patterns.

These findings provide new evidence on how vegetation associated with LEB rivers responds to rainfall and floodwater, and should assist the development, evaluation and refinement of conceptual models of how these systems function. For the riverine systems, it defines the envelope of variation under 'natural' conditions, against which potential anthropogenic impacts might be assessed. In addition, the stratification of dryland and riverine ecosystems of the South Australian LEB into regions with similar vegetation response (magnitude, timing, variability) provides a spatiotemporal context for interpreting sparse and often irregular *in-situ* measurements of physical and biological properties. This stratification could also guide and improve the efficiency and representativeness of field sampling programs. This benefit is illustrated by the interpretation of Golden Perch sample sites in relation to the temporal greenness classes (Section 5).

Analysis of past records of surface inundation derived from satellite images provided new, objective evidence of waterhole persistence after long dry periods (Section 6). Waterholes are considered important refugia for fish populations, but knowledge of their permanence, derived from field observations, is poor. Our analysis of satellite inundation records in the Neales-Peake catchment shows that only 11% of waterholes retained water through four droughts since 1999, more than half were dry at the end of all four periods, while around 40% showed different reponses after each dry period. This information helps identify core wetlands that are likely to be critical for long term species survival and can inform broader management of aquatic ecosystems in the LEB.

Analysis of the surface inundation data derived from satellite images also provided new understanding of relationships landscape processes and biological connectivity. Frequency of inundation over the past 30 years was analysed to identify flow paths through riverine systems, near-permanent waterholes and reaches and 'choke points;' where inundation is intermittent (Section 5). This information points to physical processes that influence fish dispersal and may underlie the genetic differences reported in research conducted in Task 5 of this Goyder Institute Project (Behregaray and Attard, 2015).

Throughout LEB rivers the composition of riparian vegetation is influenced by flow regimes, water salinity, substrates and climate. The presence of perennial species, in particular overstorey Eucalyptus and Acacia trees, generally indicates reliable long-term riverine flow, frequent or near permanent waterhole inundation, or access to near-surface groundwater. However, the distribution of these species is not well-documented beyond a few isolated sample sites, hence their potential for use as indicators of condition is limited. The potential for detection and mapping the distribution of Coolabah and Acacia species has been explored in this report, using airborne hyperspectral imagery and *in-situ* measurements of spectral reflectance and analytical methods suited to differentiating plants that comprise mixes of vegetative material and condition (Section 3). Subject to wider testing and accuracy assessment with more comprehensive on-ground spectral and botanical sampling, this approach shows potential for development into a method for survey and monitoring of key plant indicators of ecological condition.

Finally, this report illustrates some of the benefits to be gained from applying geographic visualisation and analysis to information derived from conventional *in-situ* sampling programs across the LEB. Examination of geographic patterns in genetic distances between Golden Perch samples reveals differences between the eastern and western fish, while analysis of independent satellite-derived information on frequency of inundation points to physical mechanisms that may underpin the population genetics (Section 5).

Interactive geographic visualisation has also enhanced access, presentation and interpretation of water quality data reported by Williams et al. (2015; Task 4 of this Goyder Institute Project). The results can be accessed and interpreted in geographic context via interactive display in Google Earth (Section 7), as a model to stimulate data sharing and encourage temporal, spatial and thematic consistency that are conducive to broader analyses.

There is considerable scope and potential benefit in developing these new approaches to encompass wider parts of the LEB, and in interpreting the new spatially-explicit indicators of ecological function and condition in conjunction with results from other studies in the Basin. Specific recommendations are made in each section of this report. Several of the indicators presented here help define envelopes of variability for unmodified LEB rivers, and could be used to identify potential impacts from anthropogenic changes in the Basin. The new landscape classifications based on riverine inundation and vegetation response provide a fuller spatiotemporal context for interpretation of sparse ecological data and could direct future on-ground sampling to achieve better spatial and temporal representation.

References

Beheregaray LB, Attard CRM (2015) Developing a Population Genomic Approach for Indicators of Environmental Condition in the Lake Eyre Basin. Goyder Institute for Water Research Technical Report Series No. 15/22, Adelaide, South Australia.

Clevers, J. G. P. W., De Jong, S. M., Epema, G. F., Van Der Meer, F. D., Bakker, W. H., and Skidmore, A. K., 2002, Derivation of the red edge index using the MERIS standard band setting, *International Journal of Remote Sensing*, 23(16): 3,169-3,184.

Cocks, T., Jenssen, R., Stewart, A., Wilson, I. and Shields, T., 1998, *The HyMap airborne hyperspectral sensor: the system, calibration and performance*, In: Proceedings of the 1st EARSeL Workshop on Imaging Spectroscopy, Eds. Schaepman, M., Schläpfer, D. and Itten, K. I., 37-43.

Crossman, S. & Li, O., 2015. Surface Hydrology Lines (National). Geoscience Australia, Canberra.

Dawson, T. P., 2000, the potential for estimating chlorophyll content from a vegetation canopy using the Medium Resolution Imaging Spectrometer (MERIS), International Journal of Remote Sensing, 21(10): 2,043-2,051.

Dawson, T. P. and Curran, P. J., 1998, A new technique for interpolating the reflectance red edge position, *International Journal of Remote Sensing*, 19(11): 2133-2139.

Dennison, P. E. and Roberts, D. A., 2003, endmember selection for multiple endmember spectral mixture analysis using endmember average RMSE, *Remote Sensing of Environment*, 87: 123-135.

Dennison, P. E., Halligan, K. Q., and Roberts, D. A., 2004, A comparison of error metrics and constraints for Multiple Endmember Spectral Mixture Analysis and Spectral Angle Mapper, *Remote Sensing of Environment*, 93: 359-367.

Dudley, K. L., Dennison, P. E., Roth, K. L., Roberts, D. A., and Coates, A. R., in press, A multi-temporal spectral library approach for mapping vegetation species across spatial and temporal phenological gradients, *Remote Sensing of Environment*.

ESRI 2011. ArcGIS Desktop: Release 10. Redlands, CA: Environmental Systems Research Institute.

Faulks, L. K., Gilligan, D. M., & Beheregaray, L. B. (2010). Islands of water in a sea of dry land: hydrological regime predicts genetic diversity and dispersal in a widespread fish from Australia's arid zone, the golden perch (Macquaria ambigua).Molecular Ecology,19(21), 4723-4737.

Geoscience Australia 2014, Landcover25 – Water (Water Observations from Space -WOfS): Product Description.

Kruse, F. A., Boardman, J. W., Lefkoff, A. B., Young, J. M. and Kierein-Young, K. S., 2000, *HyMap: an Australian hyperspectral sensor solving global problems - results from USA HyMap data acquisitions*, In: Proceedings of the International Conference Australasian Remote Sensing and Photogrammetry, 18–23. available from http://www.hyvista.com/technology/sensors [accessed: 09/02/2009].

Lewis, M.M., 2000, Discrimination of arid vegetation composition with high spectral resolution imagery. *The Rangeland Journal* 22:141-167

Lewis, M.M., Jooste, V. and de Gasparis, A.A., 2001, Discrimination of arid vegetation with Airborne Multispectral Scanner hyperspectral imagery. *IEEE Transactions on Geoscience and Remote Sensing* 39:1471-1479.

McNeil, D.G, Cheshire D.L.M, Schmarr, D.W. and Mathwin, R. (2014) A Conceptual Review of Aquatic Ecosystem Function and Fish Dynamics in the Lake Eyre Basin, Central Australia., Goyder Institute for Water Research Technical Report Series No. 15/36, Adelaide, South Australia.

Mueller, N, Lewis, A, Roberts, D, Ring, Sixsmith, JS, Lymburner, L, McIntyre, A, Tan, P, Curnow, S & Ip, A Publication in prep, Water Observations from Space: Mapping Surface Water from 25 years of Landsat Imagery across Australia.

O'Brien, E.M. (1993). Climatic gradients in woody plant species richness: Towards an explanation based on an analysis of southern Africa's woody flora. *Journal of Biogeography, 20*, 181-198

Roberts, D. A., Gardner, M., Church, R., Ustin, S., Scheer, G. and Green, R. O., 1998, Mapping chaparral in the Santa Monica mountains using Multiple Endmember Spectral Mixture Models, *Remote Sensing of Environment*, 65: 267-279.

Roberts, D. A., Dennison, P. E., Gardner, M., Hetzel, Y., Ustin, S., and Hinckley, T., 2003, Evaluation of potential of Hyperion for fire danger assessment by comparison to the airborne Visible/Infrared Imaging Spectrometer, *IEEE Transactions on Geoscience and Remote Sensing*, 41 (6 Part 1): 1,297-1,310.

Roberts, D. A., Halligan, K. Q., and Dennison, P. E., 2007, *VIPER tools user manual, version 1.5*, licensed under the Creative Commons Attribution-Non commercial-Share Alike 3.0 unported license.

Thorp, K. R., French, A. N. and Rango, A., 2013, Effect of image spatial and spectral characteristics on mapping semi-arid rangeland vegetation using multiple endmember spectral mixture analysis (MESMA, *Remote Sensing of Environment*, 132: 120-130.

White, D. C., Clarke, K. C., and Lewis, M., 2014, Mapping groundwater dependent wetland and riparian vegetation with remote sensing, DEWNR internal report.

White, D., Gotch, T., Alaak, Y., Clark, M., Ryan, J. and Lewis, M.M.,2013), Characterising spring groups. In Lewis, M.M., White, D.C. & Gotch, T.G. (Eds.). *Allocating Water and Maintaining Springs of the Western Great Artesian Basin. Volume IV. Spatial Survey and Remote Sensing of Artesian Springs of the Western Great Artesian Basin*. National Water Commission, Canberra. Pp 24-29.

Whittaker, R.J., Willis, K.J., & Field, R. (2003). Climatic-energetic explanations of diversity: A macroscopic perspective. In T.M. Blackburn & K.J. Gaston (Eds.), *Macroecology: Concepts and consequences* (pp. 107-129). Oxford: Blackwell Science

Williams M, Kookana R, Martin S, Du J, Oliver D and Cox J. 2015, *Water and sediment quality in the Diamantina-Georgina River catchment, Lake Eyre Basin.* Goyder Institute for Water Research Technical Report Series No. 15/27, Adelaide, South Australia.

Youngentob, K. N., Roberts, D. A., Held, A. A., Dennison, P. E., Jia, X., Lindenmayer, D. B., 2011, Mapping two *Eucalyptus* subgenera using multiple endmember spectral mixture analysis and continuum-removed imaging spectrometry data, *Remote Sensing of Environment*, 115(5): 1,115-1,128.

Zarco-Tejada, P. J. and Miller, J. R., 1999, Land cover mapping at BOREAS using red edge spectral parameters from CASI imagery, *Journal of Geophysical Research*, 104(D22): 27,921-27,933.

Appendices

Appendix 1: Temporal greenness class similarity table

Table 8. Distances between means and variances of pairs of combined classes, in the sequence of merging. Most similar classes were iteratively merged in pairs until a betwee-class distance of 5.83 was reached. Text in black represents class mergers which were performed, while text in light grey represents class mergers which were not performed.

Remaining class	Merged class	Between-class distance	Remaining class	Merged class	Between-class distance
24	28	3.23	35	43	4.74
6	8	3.50	11	18	4.83
2	4	3.53	10	11	4.64
13	20	3.54	22	26	4.94
31	36	3.60	22	30	4.68
38	41	3.64	6	12	5.33
15	19	3.71	40	42	5.39
11	14	3.92	1	2	5.39
18	29	4.08	10	22	5.83
42	48	4.20	35	40	6.05
10	16	4.29	35	44	5.67
13	15	4.45	35	47	5.53
5	9	4.45	31	35	5.27
23	25	4.50	31	32	6.07
26	45	4.53	10	31	6.02
33	34	4.57	5	6	6.18
11	13	4.63	27	39	6.62
11	17	4.64	7	10	7.52
37	38	4.65	5	7	7.85
31	37	4.48	3	5	7.88
31	33	4.70	3	27	8.47
18	24	4.74	3	46	9.79
18	23	4.14	1	3	12.25
18	21	4.68	1	49	14.68

Appendix 2: MESMA processing procedures

The spectral reflectance signatures of the indicator plants recorded with the field spectroradiometer and the image-based pure pixel spectra (coinciding with on-ground botanical survey plots) were pre-processed to select optimal spectra for the image analysis (spectral unmixing of the image pixels). The pre-processing used VIPER tools software (Roberts et al., 2007): the steps are summarised below.

1. Field spectra were resampled to the same configuration (number of wavebands, band widths, and wavebands influenced by atmospheric noise were also removed) as the hyperspectral imagery and visually examined for quality, poor quality spectra were removed from any further analysis;
2. Field reference spectra and image-based pure pixel spectra were compiled into several spectral libraries which were then viewed and populated with metadata (from the botanical survey recordings including vegetation cover, composition) in preparatory specialist software used for the image analysis;
3. Selection of optimal field and image spectra to perform the image analyses involved the following processing steps:
   - Computing of albedo/brightness and sorting of the spectra;
   - Convert the spectral libraries to images;
   - Creating a square array from the images;
   - Running the image spectral unmixing algorithm on the array using a number of constraints (default settings preserved - for details see image analysis section);
   - Three metrics are then calculated for determining the optimal spectra for using in the image analyses, which are Endmember Average RMSE (EAR - which locates spectra in a class which provide the best fit using RMSE; Dennison and Roberts, 2003), Minimum Average Spectral Angle (MASA - designed to select spectra with the best fit within a class using spectral angle for the fitting; Dennison et al., 2004) and Count based Endmember selection (CoB - means of selecting optimal endmembers as those members of a spectral library that model the greatest number of spectra within their class; Roberts et al., 2003); and
   - The optimal pure spectral signatures were then selected using the following criteria: EAR where the optical spectral signature has the lowest RMSE; MASA where the optimal spectral signature has the lowest average spectral angle; CoB where the optimal spectral signature has a high count-based index and high InCoB value (for details see Roberts et al., 2007).
4. Spectral unmixing parameters and constraints were selected based on those proposed by (Roberts et al. 1998), which were: fractions between -0.01 and 1.01, an RMSE threshold of 0.025, a residual threshold of 0.025 and a residual count of 7. In some cases these required modification (refer to image analysis section).

Appendix 3: Pure spectral signatures (endmembers) used for training the MESMA image analysis

The optimal image-based and field reference pure spectral signatures are presented in this Appendix. These pure endmember spectra were used in the most successful SMA and MESMA image analyses, which are presented in the Results and Discussion section of this report.

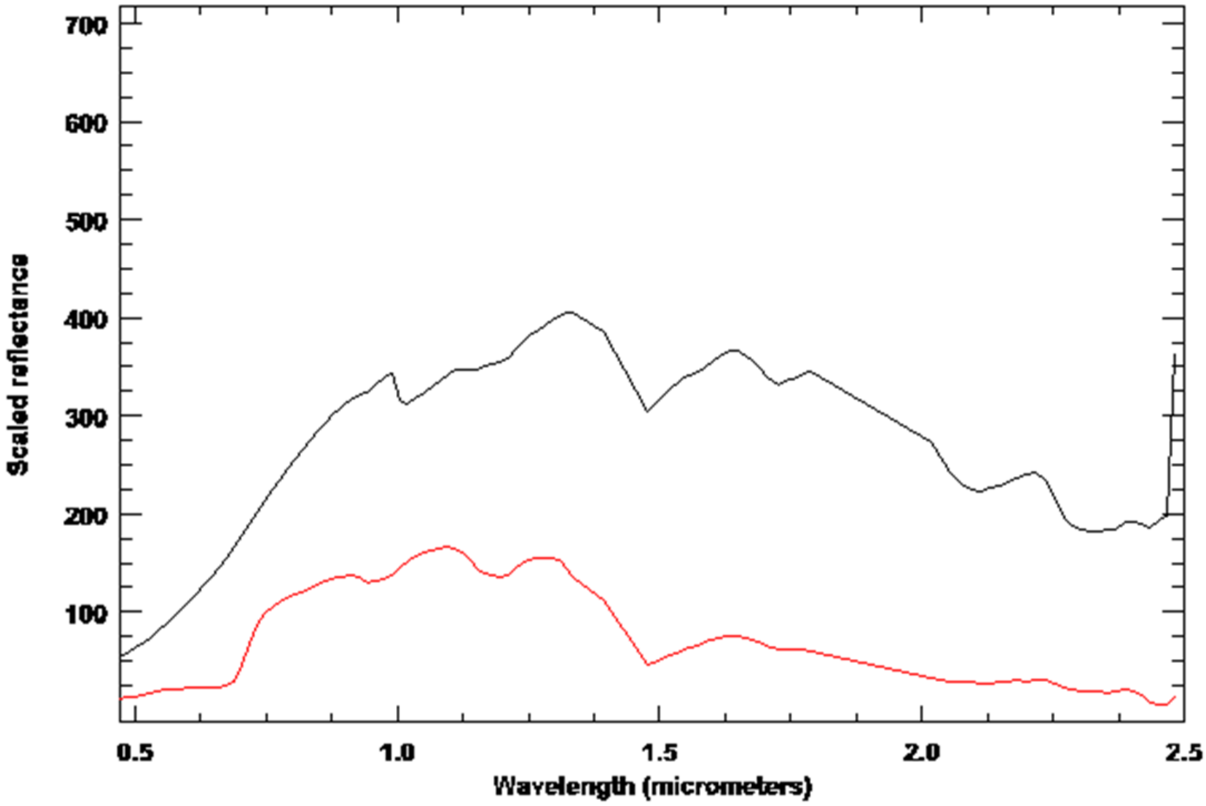

Figure 21. Spectra for photosynthetic *Eucalyptus coolabah* foliage (red spectral profile, resampled field reference spectrum, plot 43) and dry on-ground litter from *Eucalyptus coolabah* foliage (black spectral profile, resampled field reference spectrum, plot 43).

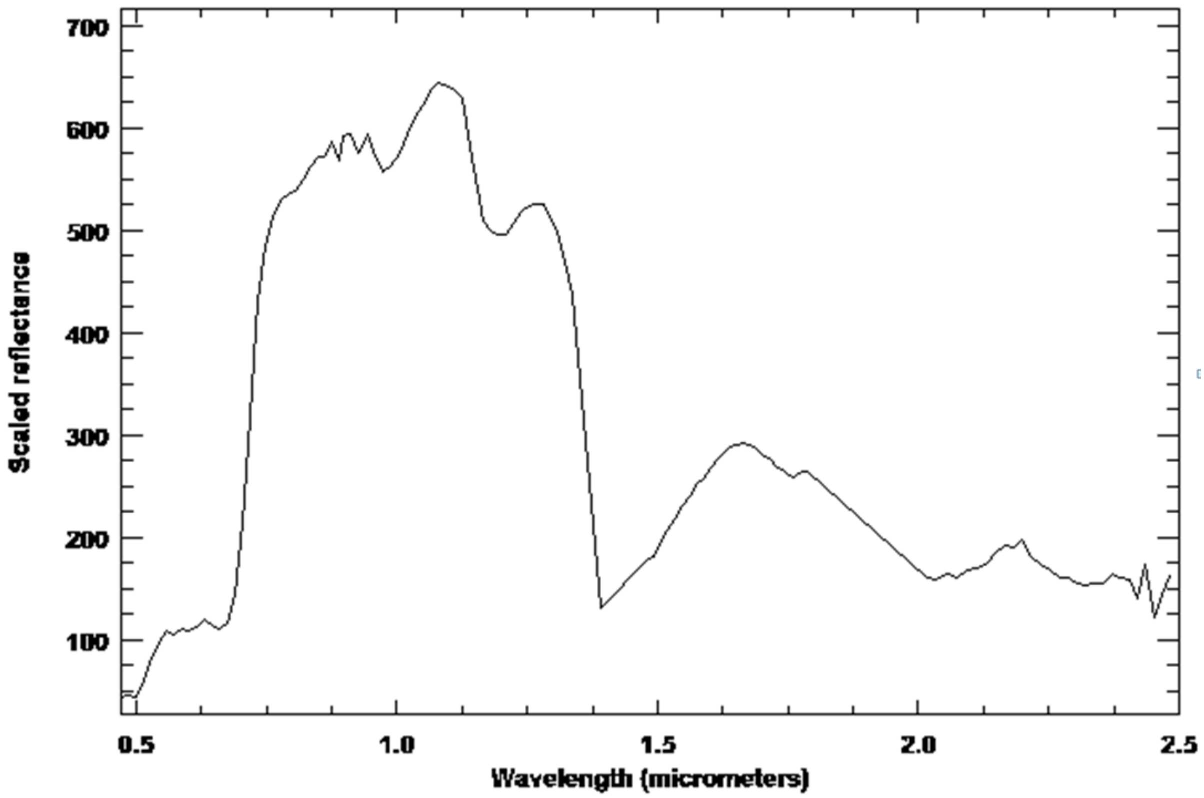

Figure 22. Spectrum for photosynthetic *Eucalyptus coolabah* foliage (image-based spectrum, plot 25).

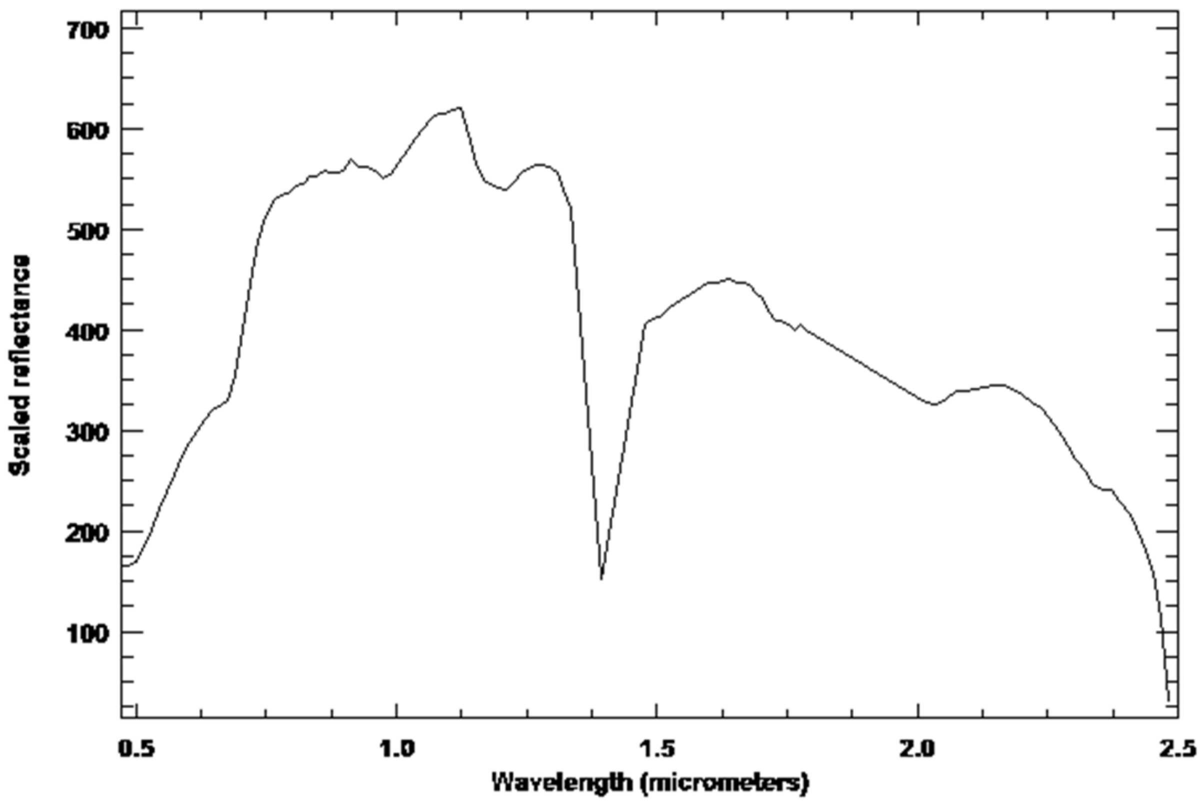

Figure 23. Spectrum for photosynthetic *Acacia cambagei* foliage (image-based spectrum, plot 46).

The Goyder Institute for Water Research is a partnership between the South Australian Government through the Department of Environment, Water and Natural Resources, CSIRO, Flinders University, the University of Adelaide and the University of South Australia.